

**CIRCULATION COPY  
SUBJECT TO RECALL  
IN TWO WEEKS**

Chemical Kinetics of the High Pressure Oxidation  
of n-Butane and its Relation to Engine Knock


William J. Pitz and Charles K. Westbrook  
Lawrence Livermore National Laboratory

This paper was prepared for submittal to  
Combustion and Flame

May 24, 1985



Lawrence  
Livermore  
National  
Laboratory



This is a preprint of a paper intended for publication in a journal or proceedings. Since changes may be made before publication, this preprint is made available with the understanding that it will not be cited or reproduced without the permission of the author.



#### DISCLAIMER

This document was prepared as an account of work sponsored by an agency of the United States Government. Neither the United States Government nor the University of California nor any of their employees, makes any warranty, express or implied, or assumes any legal liability or responsibility for the accuracy, completeness, or usefulness of any information, apparatus, product, or process disclosed, or represents that its use would not infringe privately owned rights. Reference herein to any specific commercial products, process, or service by trade name, trademark, manufacturer, or otherwise, does not necessarily constitute or imply its endorsement, recommendation, or favoring by the United States Government or the University of California. The views and opinions of authors expressed herein do not necessarily state or reflect those of the United States Government or the University of California, and shall not be used for advertising or product endorsement purposes.

**Chemical Kinetics of the High Pressure Oxidation  
of n-Butane and its Relation to Engine Knock**

William J. Pitz and Charles K. Westbrook  
Lawrence Livermore National Laboratory  
Livermore, California 94550

**ABSTRACT**

A chemical kinetic oxidation mechanism for n-butane is employed to study hydrocarbon autoignition related to engine knock. A low temperature submechanism has been added to a previously developed high temperature mechanism in order to examine the importance of low temperature reaction paths in autoignition. Numerical calculations follow reactions taking place in a sample of end gas and are used to identify the controlling chemical reactions that can lead to autoignition. Reactions that involve the production and consumption of  $\text{HO}_2$  and  $\text{H}_2\text{O}_2$  were found to play a crucial role in high pressure autoignition. A possible role of selected anti-knock additives was investigated numerically, with calculations showing that the removal of  $\text{HO}_2$  and  $\text{H}_2\text{O}_2$  by these additives would provide a strong inhibiting effect on the autoignition process.

## INTRODUCTION

Recent increases in petroleum costs have created a need to improve automotive fuel economy. This can be achieved by raising the engine compression ratio, but such increases are limited by the onset of engine knock. The anticipated introduction of lower quality and other alternative fuels into the market, as well as environmental constraints on the usage of lead anti-knock compounds, have raised concern over the resultant increase in the tendency for engines to knock. Much interest has developed concerning the chemical and physical processes that control engine knock.

Several modeling studies pertaining to engine knock have recently appeared. Leppard [1] modeled autoignition in a spark ignition engine, following measured temperatures and pressures in an engine and employing the high temperature chemical kinetic mechanism of Westbrook and Dryer [2] for ethane. He obtained good agreement (less than two crank angle degrees difference) between calculated and measured autoignition times. However, no additional reactions were added to address chemical kinetic paths that may become important at low temperatures in the engine cycle. Dimpelfeld and Foster [3] performed similar calculations for the additional fuels of  $nC_4H_{10}$ ,  $C_3H_8$ ,  $C_2H_6$ ,  $C_2H_4$ ,  $CH_4$ , and  $CH_3OH$  using both an adiabatic model which followed measured pressures in a spark ignition engine and a constant volume model. They employed the comprehensive kinetic mechanism of Westbrook and coworkers [4,5]. Halstead et al. [6] developed a multi-step overall kinetic mechanism to study autoignition of hydrocarbons. The mechanism was developed primarily to simulate some of the chemical kinetic paths occurring in the low temperature region relevant to cool flames. Using this global mechanism, Natarajan and Bracco [7] developed a

two-dimensional model to investigate engine knock and presented modeling comparisons for a constant volume bomb, rapid compression machine and stirred flow reactor. Carrier et al. [8] employed a thermal model of turbulent flame propagation to investigate processes occurring in engine knock. In their simplified model, a critical temperature was defined, with knock occurring when the end gas achieved that threshold temperature.

In spite of the considerable differences in these and other past approaches to modeling the occurrence of engine knock, there is a fairly consistent picture of the general physical and chemical events responsible for conventional engine knock. During the combustion of the fuel-air mixture in a typical spark-ignition engine, the unburned portion of the charge is subjected to a considerable increase in pressure and temperature as a result of compression both by the engine piston and by the expansion of burned product gases. During normal operation, the remaining "end-gas" is consumed by the flame propagating through the engine chamber. However, under extreme conditions of high pressure and/or temperature, it is possible for these end gases to autoignite spontaneously prior to the arrival of the flame. When autoignition produces a sufficiently rapid pressure rise and involves a significant portion of the end gas, engine knock results. The objective of the present study is to identify the controlling chemical kinetic reactions that lead to autoignition.

Although autoignition is addressed in this study, there are a number of other mechanisms which may lead to engine knock. For example, ignition of the end gas by hot spots on the combustion chamber walls and catalytic wall reactions can produce knock. Furthermore, some combustion systems have been designed to encourage engine knock, controlling the combustion to reduce or eliminate the adverse features of knock while taking advantage of

the rapid rate of heat release [9,10]. Still, the reaction paths discussed in the remainder of this paper are likely to describe the occurrence of knock in these environments as well.

## **NUMERICAL MODEL AND CHEMICAL KINETICS MECHANISM**

Numerical calculations were carried out using the HCT computer code [11] which solves the coupled conservation equations of mass, momentum, energy and each chemical species. Several different treatments for the problem boundary conditions were employed and will be discussed in detail below. The high temperature ( $T \geq 1000$  K) portion of the detailed reaction mechanism employed in the calculations (Table I) has been developed and validated in a series of previous studies [4,5]. Reverse reaction rates are computed from the forward rates and the appropriate thermodynamic data [12,13,14]. This mechanism has been shown to describe the high temperature oxidation of n-butane, propane, propene, ethane, ethylene, acetylene, methane, methanol, carbon monoxide and hydrogen over a wide range of experimental conditions.

The chemical kinetics oxidation mechanism for n-butane has been recently developed [5] and is employed here to study autoignition. N-butane is a more complex fuel than propane whose autoignition characteristics were examined in a previous paper [15]. N-butane is the simplest hydrocarbon fuel that tends to knock under conditions typically found in spark ignition engines [16,17], with a Research octane rating of 94 [18], in contrast with propane, which has a rating of 112. It also exhibits combustion chemistry characteristics that are similar to more complex hydrocarbon fuels such as primary and secondary sites for H-atom abstraction. In addition, butane occurs in another isomeric form, the

Table I  
Fuel oxidation mechanism. Reaction rates in  
cm<sup>3</sup>-mole-sec-kcal units,  $k = AT^n \exp(-E_a/RT)$

Reaction			Forward rate			Reverse rate		
			log A	n	E <sub>a</sub>	log A	n	E <sub>a</sub>
1.	H+O <sub>2</sub>	= O+OH	16.71	-0.8	16.51	13.12	0	0.68
2.	H <sub>2</sub> +O	= H+OH	10.26	1	8.90	9.92	1	6.95
3.	H <sub>2</sub> O+O	= OH+OH	13.83	0	18.35	12.80	0	1.10
4.	H <sub>2</sub> O+H	= H <sub>2</sub> +OH	13.98	0	20.30	13.34	0	5.15
5.	H <sub>2</sub> O <sub>2</sub> +OH	= H <sub>2</sub> O+HO <sub>2</sub>	13.00	0	1.80	13.45	0	32.79
6.	H <sub>2</sub> O+M	= H+OH+M	16.34	0	105.00	23.15	-2	0.00
7.	H+O <sub>2</sub> +M	= HO <sub>2</sub> +M	15.22	0	-1.00	15.36	0	45.90
8.	HO <sub>2</sub> +O	= OH+O <sub>2</sub>	13.70	0	1.00	13.81	0	56.61
9.	HO <sub>2</sub> +H	= OH+OH	14.40	0	1.90	13.08	0	40.10
10.	HO <sub>2</sub> +H	= H <sub>2</sub> +O <sub>2</sub>	13.40	0	0.70	13.74	0	57.80
11.	HO <sub>2</sub> +OH	= H <sub>2</sub> O+O <sub>2</sub>	13.70	0	1.00	14.80	0	73.86
12.	H <sub>2</sub> O <sub>2</sub> +O <sub>2</sub>	= HO <sub>2</sub> +HO <sub>2</sub>	13.60	0	42.64	13.00	0	1.00
13.	H <sub>2</sub> O <sub>2</sub> +M	= OH+OH+M	17.08	0	45.50	14.96	0	-5.07
14.	H <sub>2</sub> O <sub>2</sub> +H	= HO <sub>2</sub> +H <sub>2</sub>	12.23	0	3.75	11.86	0	18.70
15.	O+H+M	= OH+M	16.00	0	0.00	19.90	-1	103.72
16.	O <sub>2</sub> +M	= O+O+M	15.71	0	115.00	15.67	-0.28	0.00
17.	H <sub>2</sub> +M	= H+H+M	14.34	0	96.00	15.48	0	0.00
18.	CO+OH	= CO <sub>2</sub> +H	7.18	1.3	-0.77	9.23	1.3	21.58
19.	CO+HO <sub>2</sub>	= CO <sub>2</sub> +OH	14.18	0	23.65	15.23	0	85.50
20.	CO+O+M	= CO <sub>2</sub> +M	15.77	0	4.10	21.74	-1	131.78
21.	CO <sub>2</sub> +O	= CO+O <sub>2</sub>	12.44	0	43.83	11.50	0	37.60
22.	HCO+OH	= CO+H <sub>2</sub> O	14.00	0	0.00	15.45	0	105.15
23.	HCO+M	= H+CO+M	14.16	0	19.00	11.70	1	1.55
24.	HCO+H	= CO+H <sub>2</sub>	14.30	0	0.00	15.12	0	90.00
25.	HCO+O	= CO+OH	14.00	0	0.00	14.46	0	87.90
26.	HCO+HO <sub>2</sub>	= CH <sub>2</sub> O+O <sub>2</sub>	14.00	0	3.00	15.56	0	46.04
27.	HCO+O <sub>2</sub>	= CO+HO <sub>2</sub>	12.48	0	0.00	12.83	0	32.29
28.	CH <sub>2</sub> O+M	= HCO+H+M	16.52	0	81.00	11.15	1	-11.77
29.	CH <sub>2</sub> O+OH	= HCO+H <sub>2</sub> O	12.88	0	0.17	12.41	0	30.00
30.	CH <sub>2</sub> O+H	= HCO+H <sub>2</sub>	14.52	0	10.50	13.42	0	25.17
31.	CH <sub>2</sub> O+O	= HCO+OH	13.70	0	4.60	12.24	0	17.17
32.	CH <sub>2</sub> O+HO <sub>2</sub>	= HCO+H <sub>2</sub> O <sub>2</sub>	11.30	0	8.00	10.34	0	6.59
33.	CH <sub>4</sub> +M	= CH <sub>3</sub> +H+M	17.15	0	88.40	11.45	1	-19.52
34.	CH <sub>4</sub> +H	= CH <sub>3</sub> +H <sub>2</sub>	14.10	0	11.90	12.68	0	11.43
35.	CH <sub>4</sub> +OH	= CH <sub>3</sub> +H <sub>2</sub> O	3.54	3.08	2.00	2.76	3.08	16.68
36.	CH <sub>4</sub> +O	= CH <sub>3</sub> +OH	6.33	2.21	6.48	4.55	2.21	3.92
37.	CH <sub>4</sub> +HO <sub>2</sub>	= CH <sub>3</sub> +H <sub>2</sub> O <sub>2</sub>	13.30	0	18.00	11.50	0	8.00
38.	CH <sub>3</sub> +HO <sub>2</sub>	= CH <sub>3</sub> O+OH	13.51	0	0.00	10.30	0	0.00
39.	CH <sub>3</sub> +OH	= CH <sub>2</sub> O+H <sub>2</sub>	12.60	0	0.00	14.08	0	71.73
40.	CH <sub>3</sub> +O	= CH <sub>2</sub> O+H	14.11	0	2.00	15.23	0	71.63
41.	CH <sub>3</sub> +O <sub>2</sub>	= CH <sub>3</sub> O+O	13.68	0	29.00	14.48	0	0.73
42.	CH <sub>2</sub> O+CH <sub>3</sub>	= CH <sub>4</sub> +HCO	10.00	0.5	6.00	10.32	0.5	21.14
43.	CH <sub>3</sub> +HCO	= CH <sub>4</sub> +CO	11.48	0.5	0.00	13.71	0.5	90.47
44.	CH <sub>3</sub> +HO <sub>2</sub>	= CH <sub>4</sub> +O <sub>2</sub>	12.00	0	0.40	13.88	0	58.59
45.	CH <sub>3</sub> O+M	= CH <sub>2</sub> O+H+M	13.70	0	21.00	9.00	1	-2.56
46.	CH <sub>3</sub> O+O <sub>2</sub>	= CH <sub>2</sub> O+HO <sub>2</sub>	10.88	0	2.70	10.00	0	28.87
47.	C <sub>2</sub> H <sub>6</sub>	= CH <sub>3</sub> +CH <sub>3</sub>	19.35	-1	88.31	12.95	0	0.00
48.	C <sub>2</sub> H <sub>6</sub> +CH <sub>3</sub>	= C <sub>2</sub> H <sub>5</sub> +CH <sub>4</sub>	-0.26	4	8.28	10.48	0	12.50

Table I (continued)  
Fuel oxidation mechanism. Reaction rates in  
cm<sup>3</sup>-mole-sec-kcal units,  $k = AT^n \exp(-E_a/RT)$

Reaction			Forward rate			Reverse rate		
			log A	n	E <sub>a</sub>	log A	n	E <sub>a</sub>
49.	C <sub>2</sub> H <sub>6</sub> +H	= C <sub>2</sub> H <sub>5</sub> +H <sub>2</sub>	2.73	3.5	5.20	2.99	3.5	27.32
50.	C <sub>2</sub> H <sub>6</sub> +OH	= C <sub>2</sub> H <sub>5</sub> +H <sub>2</sub> O	9.94	1.05	1.81	10.23	1.05	23.94
51.	C <sub>2</sub> H <sub>6</sub> +O	= C <sub>2</sub> H <sub>5</sub> +OH	14.05	0	7.85	13.32	0	12.72
52.	C <sub>2</sub> H <sub>5</sub> +M	= C <sub>2</sub> H <sub>4</sub> +H+M	15.30	0	30.00	10.62	0	-11.03
53.	C <sub>2</sub> H <sub>5</sub> +O <sub>2</sub>	= C <sub>2</sub> H <sub>4</sub> +HO <sub>2</sub>	12.00	0	5.00	11.12	0	13.70
54.	C <sub>2</sub> H <sub>4</sub> +C <sub>2</sub> H <sub>4</sub>	= C <sub>2</sub> H <sub>5</sub> +C <sub>2</sub> H <sub>3</sub>	14.70	0	64.70	12.48	0	0.00
55.	C <sub>2</sub> H <sub>4</sub> +M	= C <sub>2</sub> H <sub>2</sub> +H <sub>2</sub>	16.97	0	77.20	12.66	1	36.52
56.	C <sub>2</sub> H <sub>4</sub> +M	= C <sub>2</sub> H <sub>3</sub> +H+M	18.80	0	108.72	17.30	0	0.00
57.	C <sub>2</sub> H <sub>4</sub> +O	= CH <sub>3</sub> +HCO	12.52	0	1.13	11.20	0	31.18
58.	C <sub>2</sub> H <sub>4</sub> +O	= CH <sub>2</sub> O+CH <sub>2</sub>	13.40	0	5.00	12.48	0	15.68
59.	C <sub>2</sub> H <sub>4</sub> +H	= C <sub>2</sub> H <sub>3</sub> +H <sub>2</sub>	7.18	2	6.00	6.24	2	5.11
60.	C <sub>2</sub> H <sub>4</sub> +OH	= C <sub>2</sub> H <sub>3</sub> +H <sub>2</sub> O	12.68	0	1.23	12.08	0	14.00
61.	C <sub>2</sub> H <sub>4</sub> +OH	= CH <sub>3</sub> +CH <sub>2</sub> O	12.30	0	0.96	11.78	0	16.48
62.	C <sub>2</sub> H <sub>3</sub> +M	= C <sub>2</sub> H <sub>2</sub> +H+M	14.90	0	31.50	11.09	1	-10.36
63.	C <sub>2</sub> H <sub>3</sub> +O <sub>2</sub>	= C <sub>2</sub> H <sub>2</sub> +HO <sub>2</sub>	12.00	0	10.00	12.00	0	17.87
64.	C <sub>2</sub> H <sub>2</sub> +M	= C <sub>2</sub> H+H+M	14.00	0	114.00	9.04	1	0.77
65.	C <sub>2</sub> H <sub>2</sub> +O <sub>2</sub>	= HCO+HCO	12.60	0	28.00	11.00	0	63.65
66.	C <sub>2</sub> H <sub>2</sub> +H	= C <sub>2</sub> H+H <sub>2</sub>	14.30	0	19.00	13.62	0	13.21
67.	C <sub>2</sub> H <sub>2</sub> +OH	= C <sub>2</sub> H+H <sub>2</sub> O	12.78	0	7.00	12.73	0	16.36
68.	C <sub>2</sub> H <sub>2</sub> +OH	= CH <sub>2</sub> CO+H	11.51	0	0.20	12.50	0	20.87
69.	C <sub>2</sub> H <sub>2</sub> +O	= C <sub>2</sub> H+OH	15.51	-0.6	17.00	14.47	-0.6	0.91
70.	C <sub>2</sub> H <sub>2</sub> +O	= CH <sub>2</sub> +CO	13.83	0	4.00	13.10	0	54.67
71.	C <sub>2</sub> H+O <sub>2</sub>	= HCO+CO	13.00	0	7.00	12.93	0	138.40
72.	C <sub>2</sub> H+O	= CO+CH	13.70	0	0.00	13.50	0	59.43
73.	CH <sub>2</sub> +O <sub>2</sub>	= HCO+OH	14.00	0	3.70	13.61	0	76.58
74.	CH <sub>2</sub> +O	= CH+OH	11.28	0.68	25.00	10.77	0.68	25.93
75.	CH <sub>2</sub> +H	= CH+H <sub>2</sub>	11.43	0.67	25.70	11.28	0.67	28.72
76.	CH <sub>2</sub> +OH	= CH+H <sub>2</sub> O	11.43	0.67	25.70	11.91	0.67	43.88
77.	CH+O <sub>2</sub>	= CO+OH	11.13	0.67	25.70	11.71	0.67	185.60
78.	CH+O <sub>2</sub>	= HCO+O	13.00	0	0.00	13.13	0	71.95
79.	CH <sub>3</sub> OH+M	= CH <sub>3</sub> +OH+M	18.48	0	80.00	13.16	1	-10.98
80.	CH <sub>3</sub> OH+OH	= CH <sub>2</sub> OH+H <sub>2</sub> O	12.60	0	1.37	7.27	1.66	24.68
81.	CH <sub>3</sub> OH+O	= CH <sub>2</sub> OH+OH	12.23	0	2.29	5.90	1.66	8.35
82.	CH <sub>3</sub> OH+H	= CH <sub>2</sub> OH+H <sub>2</sub>	13.48	0	7.00	7.51	1.66	15.16
83.	CH <sub>3</sub> OH+H	= CH <sub>3</sub> +H <sub>2</sub> O	12.72	0	5.34	12.32	0	36.95
84.	CH <sub>3</sub> OH+CH <sub>3</sub>	= CH <sub>2</sub> OH+CH <sub>4</sub>	11.26	0	9.80	6.70	1.66	18.43
85.	CH <sub>3</sub> OH+HO <sub>2</sub>	= CH <sub>2</sub> OH+H <sub>2</sub> O <sub>2</sub>	12.80	0	19.36	7.00	1.66	11.44
86.	CH <sub>2</sub> OH+M	= CH <sub>2</sub> O+H+M	13.40	0	29.00	16.69	-0.66	7.58
87.	CH <sub>2</sub> OH+O <sub>2</sub>	= CH <sub>2</sub> O+HO <sub>2</sub>	11.92	0	0.00	17.94	-1.66	22.32
88.	C <sub>2</sub> H <sub>3</sub> +C <sub>2</sub> H <sub>4</sub>	= C <sub>4</sub> H <sub>6</sub> +H	11.70	0	7.30	13.00	0	4.70
89.	C <sub>2</sub> H <sub>2</sub> +C <sub>2</sub> H <sub>2</sub>	= C <sub>4</sub> H <sub>3</sub> +H	13.00	0	45.00	13.18	0	0.00
90.	C <sub>4</sub> H <sub>3</sub> +M	= C <sub>4</sub> H <sub>2</sub> +H+M	16.00	0	60.00	11.92	1	2.54
91.	C <sub>2</sub> H <sub>2</sub> +C <sub>2</sub> H	= C <sub>4</sub> H <sub>2</sub> +H	13.60	0	0.00	14.65	0	0.55
92.	C <sub>4</sub> H <sub>2</sub> +M	= C <sub>4</sub> H+H+M	17.54	0	80.00	12.30	1.0	-16.40
93.	C <sub>2</sub> H <sub>3</sub> +H	= C <sub>2</sub> H <sub>2</sub> +H <sub>2</sub>	13.30	0	2.50	13.12	0	68.08
94.	C <sub>3</sub> H <sub>8</sub>	= CH <sub>3</sub> +C <sub>2</sub> H <sub>5</sub>	16.23	0	84.84	10.18	1	-0.32
95.	CH <sub>3</sub> +C <sub>3</sub> H <sub>8</sub>	= CH <sub>4</sub> +iC <sub>3</sub> H <sub>7</sub>	15.04	0	25.14	15.64	0	32.12
96.	CH <sub>3</sub> +C <sub>3</sub> H <sub>8</sub>	= CH <sub>4</sub> +nC <sub>3</sub> H <sub>7</sub>	15.04	0	25.14	15.64	0	32.12



Table I (continued)  
 Fuel oxidation mechanism. Reaction rates in  
 $\text{cm}^3\text{-mole-sec-kcal units, } k = AT^n \exp(-E_a/RT)$

	Reaction	Forward rate			Reverse rate		
		log A	n	$E_a$	log A	n	$E_a$
97.	$\text{H} + \text{C}_3\text{H}_8 = \text{H}_2 + \text{iC}_3\text{H}_7$	6.94	2	5.00	12.89	0	15.87
98.	$\text{H} + \text{C}_3\text{H}_8 = \text{H}_2 + \text{nC}_3\text{H}_7$	7.75	2	7.70	12.96	0	14.46
99.	$\text{iC}_3\text{H}_7 = \text{H} + \text{C}_3\text{H}_6$	13.80	0	36.90	13.00	0	1.50
100.	$\text{iC}_3\text{H}_7 = \text{CH}_3 + \text{C}_2\text{H}_4$	10.30	0	29.50	4.66	1	4.29
101.	$\text{nC}_3\text{H}_7 = \text{CH}_3 + \text{C}_2\text{H}_4$	13.98	0	31.00	8.34	1	5.79
102.	$\text{nC}_3\text{H}_7 = \text{H} + \text{C}_3\text{H}_6$	14.10	0	37.00	13.00	0	1.50
103.	$\text{iC}_3\text{H}_7 + \text{C}_3\text{H}_8 = \text{nC}_3\text{H}_7 + \text{C}_3\text{H}_8$	10.48	0	12.90	10.48	0	12.90
104.	$\text{C}_2\text{H}_3 + \text{C}_3\text{H}_8 = \text{C}_2\text{H}_4 + \text{iC}_3\text{H}_7$	11.00	0	10.40	11.12	0	17.80
105.	$\text{C}_2\text{H}_3 + \text{C}_3\text{H}_8 = \text{C}_2\text{H}_4 + \text{nC}_3\text{H}_7$	11.00	0	10.40	11.12	0	17.80
106.	$\text{C}_2\text{H}_5 + \text{C}_3\text{H}_8 = \text{C}_2\text{H}_6 + \text{iC}_3\text{H}_7$	11.00	0	10.40	10.56	0	9.93
107.	$\text{C}_2\text{H}_5 + \text{C}_3\text{H}_8 = \text{C}_2\text{H}_6 + \text{nC}_3\text{H}_7$	11.00	0	10.40	10.56	0	9.93
108.	$\text{C}_3\text{H}_8 + \text{O} = \text{iC}_3\text{H}_7 + \text{OH}$	13.45	0	5.20	12.27	0	9.61
109.	$\text{C}_3\text{H}_8 + \text{O} = \text{nC}_3\text{H}_7 + \text{OH}$	14.05	0	7.85	12.88	0	12.26
110.	$\text{C}_3\text{H}_8 + \text{OH} = \text{iC}_3\text{H}_7 + \text{H}_2\text{O}$	8.68	1.4	0.85	8.93	1.25	22.37
111.	$\text{C}_3\text{H}_8 + \text{OH} = \text{nC}_3\text{H}_7 + \text{H}_2\text{O}$	8.76	1.4	0.85	9.01	1.25	22.37
112.	$\text{C}_3\text{H}_8 + \text{HO}_2 = \text{iC}_3\text{H}_7 + \text{H}_2\text{O}_2$	12.53	0	17.00	11.84	0	7.43
113.	$\text{C}_3\text{H}_8 + \text{HO}_2 = \text{nC}_3\text{H}_7 + \text{H}_2\text{O}_2$	13.05	0	19.40	12.37	0	9.83
114.	$\text{C}_3\text{H}_6 + \text{O} = \text{C}_2\text{H}_4 + \text{CH}_2\text{O}$	4.83	2.56	-1.13	4.82	2.56	80.54
115.	$\text{iC}_3\text{H}_7 + \text{O}_2 = \text{C}_3\text{H}_6 + \text{HO}_2$	12.00	0	5.00	11.30	0	17.48
116.	$\text{nC}_3\text{H}_7 + \text{O}_2 = \text{C}_3\text{H}_6 + \text{HO}_2$	12.00	0	5.00	11.30	0	17.48
117.	$\text{C}_3\text{H}_8 + \text{O}_2 = \text{iC}_3\text{H}_7 + \text{HO}_2$	13.60	0	47.50	12.31	0	0.00
118.	$\text{C}_3\text{H}_8 + \text{O}_2 = \text{nC}_3\text{H}_7 + \text{HO}_2$	13.60	0	47.50	12.31	0	0.00
119.	$\text{C}_3\text{H}_6 + \text{OH} = \text{C}_2\text{H}_5 + \text{CH}_2\text{O}$	12.00	0	0.00	12.76	0	17.35
120.	$\text{C}_3\text{H}_6 + \text{O} = \text{C}_2\text{H}_5 + \text{HCO}$	4.83	2.56	-1.13	4.13	2.56	28.79
121.	$\text{C}_3\text{H}_6 + \text{OH} = \text{CH}_3 + \text{CH}_3\text{CHO}$	12.00	0	0.00	11.50	0	20.40
122.	$\text{C}_3\text{H}_6 + \text{O} = \text{CH}_3 + \text{CH}_3\text{CO}$	4.83	2.56	-1.13	4.01	2.56	36.64
123.	$\text{CH}_3\text{CHO} + \text{H} = \text{CH}_3\text{CO} + \text{H}_2$	13.60	0	4.20	13.25	0	23.67
124.	$\text{CH}_3\text{CHO} + \text{OH} = \text{CH}_3\text{CO} + \text{H}_2\text{O}$	13.00	0	0.00	13.28	0	36.62
125.	$\text{CH}_3\text{CHO} + \text{O} = \text{CH}_3\text{CO} + \text{OH}$	12.70	0	1.79	12.00	0	19.16
126.	$\text{CH}_3\text{CHO} + \text{CH}_3 = \text{CH}_3\text{CO} + \text{CH}_4$	12.24	0	8.44	13.54	0	28.44
127.	$\text{CH}_3\text{CHO} + \text{HO}_2 = \text{CH}_3\text{CO} + \text{H}_2\text{O}_2$	12.23	0	10.70	12.00	0	14.10
128.	$\text{CH}_3\text{CHO} = \text{CH}_3 + \text{HCO}$	15.85	0	81.78	9.58	1	0.00
129.	$\text{CH}_3\text{CHO} + \text{O}_2 = \text{CH}_3\text{CO} + \text{HO}_2$	13.30	0.5	42.20	7.00	0.5	4.00
130.	$\text{CH}_3\text{CO} + \text{M} = \text{CH}_3 + \text{CO} + \text{M}$	15.64	0	10.50	11.20	0	5.97
131.	$\text{C}_3\text{H}_6 + \text{H} = \text{C}_3\text{H}_5 + \text{H}_2$	12.70	0	1.50	12.18	0	17.70
132.	$\text{C}_3\text{H}_6 + \text{CH}_3 = \text{C}_3\text{H}_5 + \text{CH}_4$	12.20	0	8.80	13.12	0	25.48
133.	$\text{C}_3\text{H}_6 + \text{C}_2\text{H}_5 = \text{C}_3\text{H}_5 + \text{C}_2\text{H}_6$	11.00	0	9.80	11.90	0	20.50
134.	$\text{C}_3\text{H}_6 + \text{OH} = \text{C}_3\text{H}_5 + \text{H}_2\text{O}$	13.00	0	3.06	7.58	0	72.75
135.	$\text{C}_3\text{H}_8 + \text{C}_3\text{H}_5 = \text{iC}_3\text{H}_7 + \text{C}_3\text{H}_6$	11.30	0	16.10	10.60	0	9.70
136.	$\text{C}_3\text{H}_8 + \text{C}_3\text{H}_5 = \text{nC}_3\text{H}_7 + \text{C}_3\text{H}_6$	11.90	0	20.50	11.00	0	9.80
137.	$\text{C}_3\text{H}_5 = \text{C}_3\text{H}_4 + \text{H}$	13.60	0	70.00	8.00	1	0.00
138.	$\text{C}_3\text{H}_5 + \text{O}_2 = \text{C}_3\text{H}_4 + \text{HO}_2$	11.78	0	10.00	11.08	0	10.00
139.	$1\text{C}_4\text{H}_8 = \text{C}_3\text{H}_5 + \text{CH}_3$	19.18	-1	73.40	13.13	0	0.00
140.	$1\text{C}_4\text{H}_8 = \text{C}_2\text{H}_3 + \text{C}_2\text{H}_5$	19.00	-1	96.77	12.95	0	0.00
141.	$1\text{C}_4\text{H}_8 + \text{O} = \text{CH}_3\text{CHO} + \text{C}_2\text{H}_4$	13.11	0	0.85	12.32	0	85.10
142.	$1\text{C}_4\text{H}_8 + \text{O} = \text{CH}_3\text{CO} + \text{C}_2\text{H}_5$	13.11	0	0.85	12.37	0	38.15
143.	$1\text{C}_4\text{H}_8 + \text{OH} = \text{CH}_3\text{CHO} + \text{C}_2\text{H}_5$	11.00	0	0.00	10.97	0	19.93
144.	$1\text{C}_4\text{H}_8 + \text{OH} = \text{CH}_3\text{CO} + \text{C}_2\text{H}_6$	10.00	0	0.00	9.99	0	32.43

Table I (continued)  
Fuel oxidation mechanism. Reaction rates in  
cm<sup>3</sup>-mole-sec-kcal units,  $k = AT^n \exp(-E_a/RT)$

Reaction			Forward rate			Reverse rate		
			log A	n	E <sub>a</sub>	log A	n	E <sub>a</sub>
145.	C <sub>3</sub> H <sub>4</sub> +O	= CH <sub>2</sub> O+C <sub>2</sub> H <sub>2</sub>	12.00	0	0.00	12.03	0	81.73
146.	C <sub>3</sub> H <sub>4</sub> +O	= HCO+C <sub>2</sub> H <sub>3</sub>	12.00	0	0.00	10.47	0	30.82
147.	C <sub>3</sub> H <sub>4</sub> +OH	= CH <sub>2</sub> O+C <sub>2</sub> H <sub>3</sub>	12.00	0	0.00	11.93	0	18.25
148.	C <sub>3</sub> H <sub>4</sub> +OH	= HCO+C <sub>2</sub> H <sub>4</sub>	12.00	0	0.00	11.77	0	33.81
149.	C <sub>3</sub> H <sub>6</sub>	= C <sub>3</sub> H <sub>5</sub> +H	13.00	0	78.00	11.00	0	0.00
150.	C <sub>2</sub> H <sub>2</sub> +O	= HCCO+H	4.55	2.7	1.39	2.70	2.7	12.79
151.	CH <sub>2</sub> CO+H	= CH <sub>3</sub> +CO	13.04	0	3.40	12.38	0	40.20
152.	CH <sub>2</sub> CO+O	= HCO+HCO	13.00	0	2.40	11.54	0	33.50
153.	CH <sub>2</sub> CO+OH	= CH <sub>2</sub> O+HCO	13.45	0	0.00	13.44	0	18.50
154.	CH <sub>2</sub> CO+M	= CH <sub>2</sub> +CO+M	16.30	0	60.00	10.66	0	0.00
155.	CH <sub>2</sub> CO+O	= HCCO+OH	13.70	0	8.00	10.86	0	8.00
156.	CH <sub>2</sub> CO+OH	= HCCO+H <sub>2</sub> O	12.88	0	3.00	11.03	0	11.00
157.	CH <sub>2</sub> CO+H	= HCCO+H <sub>2</sub>	13.88	0	8.00	11.39	0	8.00
158.	HCCO+OH	= HCO+HCO	13.00	0	0.00	13.68	0	40.36
159.	HCCO+H	= CH <sub>2</sub> +CO	13.70	0	0.00	13.82	0	39.26
160.	HCCO+O	= HCO+CO	13.53	0	2.00	13.92	0	128.26
161.	C <sub>3</sub> H <sub>6</sub>	= C <sub>2</sub> H <sub>3</sub> +CH <sub>3</sub>	15.80	0	85.80	10.00	1	0.00
162.	C <sub>3</sub> H <sub>5</sub> +H	= C <sub>3</sub> H <sub>4</sub> +H <sub>2</sub>	13.00	0	0.00	13.00	0	40.00
163.	C <sub>3</sub> H <sub>5</sub> +CH <sub>3</sub>	= C <sub>3</sub> H <sub>4</sub> +CH <sub>4</sub>	12.00	0	0.00	13.00	0	40.00
164.	C <sub>2</sub> H <sub>6</sub> +O <sub>2</sub>	= C <sub>2</sub> H <sub>5</sub> +HO <sub>2</sub>	13.00	0	51.00	12.37	0	2.00
165.	C <sub>2</sub> H <sub>6</sub> +HO <sub>2</sub>	= C <sub>2</sub> H <sub>5</sub> +H <sub>2</sub> O <sub>2</sub>	13.05	0	19.40	12.81	0	10.29
166.	CH <sub>3</sub> +C <sub>2</sub> H <sub>3</sub>	= CH <sub>4</sub> +C <sub>2</sub> H <sub>2</sub>	12.00	0	0.00	13.88	0	65.05
167.	CH <sub>3</sub> +C <sub>2</sub> H <sub>5</sub>	= CH <sub>4</sub> +C <sub>2</sub> H <sub>4</sub>	11.90	0	0.00	12.91	0	66.89
168.	C <sub>2</sub> H <sub>5</sub> +C <sub>3</sub> H <sub>5</sub>	= C <sub>3</sub> H <sub>6</sub> +C <sub>2</sub> H <sub>4</sub>	12.10	0	0.00	10.00	0	50.00
169.	C <sub>2</sub> H <sub>5</sub> +C <sub>2</sub> H <sub>5</sub>	= C <sub>2</sub> H <sub>6</sub> +C <sub>2</sub> H <sub>4</sub>	11.70	0	0.00	11.70	0	60.00
170.	CH <sub>3</sub> OH+CH <sub>2</sub> O	= CH <sub>3</sub> O+CH <sub>3</sub> O	12.19	0	79.57	13.48	0	0.00
171.	CH <sub>2</sub> O+CH <sub>3</sub> O	= CH <sub>3</sub> OH+HCO	11.78	0	3.30	9.82	0	13.67
172.	CH <sub>4</sub> +CH <sub>3</sub> O	= CH <sub>3</sub> OH+CH <sub>3</sub>	11.30	0	7.00	9.02	0	2.22
173.	C <sub>2</sub> H <sub>6</sub> +CH <sub>3</sub> O	= CH <sub>3</sub> OH+C <sub>2</sub> H <sub>5</sub>	11.48	0	7.00	10.23	0	9.67
174.	C <sub>3</sub> H <sub>8</sub> +CH <sub>3</sub> O	= CH <sub>3</sub> OH+iC <sub>3</sub> H <sub>7</sub>	11.48	0	7.00	10.23	0	9.67
175.	C <sub>3</sub> H <sub>8</sub> +CH <sub>3</sub> O	= CH <sub>3</sub> OH+nC <sub>3</sub> H <sub>7</sub>	11.48	0	7.00	10.23	0	9.67
176.	C <sub>4</sub> H <sub>10</sub>	= C <sub>2</sub> H <sub>5</sub> +C <sub>2</sub> H <sub>5</sub>	16.30	0	81.30	12.60	0	0.00
177.	C <sub>4</sub> H <sub>10</sub>	= nC <sub>3</sub> H <sub>7</sub> +CH <sub>3</sub>	17.00	0	85.40	13.30	0	0.00
178.	C <sub>4</sub> H <sub>10</sub> +O <sub>2</sub>	= pC <sub>4</sub> H <sub>9</sub> +HO <sub>2</sub>	13.40	0	49.00	12.40	0	-2.20
179.	C <sub>4</sub> H <sub>10</sub> +O <sub>2</sub>	= sC <sub>4</sub> H <sub>9</sub> +HO <sub>2</sub>	13.60	0	47.60	12.61	0	-3.62
180.	C <sub>4</sub> H <sub>10</sub> +H	= pC <sub>4</sub> H <sub>9</sub> +H <sub>2</sub>	7.75	2	7.70	12.96	0	14.46
181.	C <sub>4</sub> H <sub>10</sub> +H	= sC <sub>4</sub> H <sub>9</sub> +H <sub>2</sub>	7.24	2	5.00	13.19	0	15.87
182.	C <sub>4</sub> H <sub>10</sub> +OH	= pC <sub>4</sub> H <sub>9</sub> +H <sub>2</sub> O	9.94	1.05	1.81	10.17	1.05	23.33
183.	C <sub>4</sub> H <sub>10</sub> +OH	= sC <sub>4</sub> H <sub>9</sub> +H <sub>2</sub> O	9.41	1.25	0.70	9.66	1.25	22.22
184.	C <sub>4</sub> H <sub>10</sub> +O	= pC <sub>4</sub> H <sub>9</sub> +OH	14.05	0	7.85	13.17	0	12.24
185.	C <sub>4</sub> H <sub>10</sub> +O	= sC <sub>4</sub> H <sub>9</sub> +OH	13.75	0	5.20	12.87	0	9.59
186.	C <sub>4</sub> H <sub>10</sub> +CH <sub>3</sub>	= pC <sub>4</sub> H <sub>9</sub> +CH <sub>4</sub>	12.11	0	11.60	13.00	0	18.56
187.	C <sub>4</sub> H <sub>10</sub> +CH <sub>3</sub>	= sC <sub>4</sub> H <sub>9</sub> +CH <sub>4</sub>	11.90	0	9.50	12.80	0	16.46
188.	C <sub>4</sub> H <sub>10</sub> +C <sub>2</sub> H <sub>3</sub>	= pC <sub>4</sub> H <sub>9</sub> +C <sub>2</sub> H <sub>4</sub>	12.00	0	18.00	12.41	0	25.38
189.	C <sub>4</sub> H <sub>10</sub> +C <sub>2</sub> H <sub>3</sub>	= sC <sub>4</sub> H <sub>9</sub> +C <sub>2</sub> H <sub>4</sub>	11.90	0	16.80	12.31	0	24.18
190.	C <sub>4</sub> H <sub>10</sub> +C <sub>2</sub> H <sub>5</sub>	= pC <sub>4</sub> H <sub>9</sub> +C <sub>2</sub> H <sub>6</sub>	11.00	0	13.40	10.85	0	12.92
191.	C <sub>4</sub> H <sub>10</sub> +C <sub>2</sub> H <sub>5</sub>	= sC <sub>4</sub> H <sub>9</sub> +C <sub>2</sub> H <sub>6</sub>	11.00	0	10.40	10.85	0	9.92
192.	C <sub>4</sub> H <sub>10</sub> +C <sub>3</sub> H <sub>5</sub>	= pC <sub>4</sub> H <sub>9</sub> +C <sub>3</sub> H <sub>6</sub>	11.90	0	20.50	11.00	0	9.80

Table I (continued)  
 Fuel oxidation mechanism. Reaction rates in  
 $\text{cm}^3\text{-mole-sec-kcal}$  units,  $k = AT^n \exp(-E_a/RT)$

Reaction			Forward rate			Reverse rate		
			log A	n	$E_a$	log A	n	$E_a$
193.	$\text{C}_4\text{H}_{10} + \text{C}_3\text{H}_5$	$= \text{sC}_4\text{H}_9 + \text{C}_3\text{H}_6$	11.50	0	16.40	10.60	0	9.70
194.	$\text{C}_4\text{H}_{10} + \text{HO}_2$	$= \text{pC}_4\text{H}_9 + \text{H}_2\text{O}_2$	13.05	0	19.40	12.66	0	9.81
195.	$\text{C}_4\text{H}_{10} + \text{HO}_2$	$= \text{sC}_4\text{H}_9 + \text{H}_2\text{O}_2$	12.83	0	17.00	12.44	0	7.41
196.	$\text{C}_4\text{H}_{10} + \text{CH}_3\text{O}$	$= \text{pC}_4\text{H}_9 + \text{CH}_3\text{OH}$	11.48	0	7.00	10.09	0	9.18
197.	$\text{C}_4\text{H}_{10} + \text{CH}_3\text{O}$	$= \text{sC}_4\text{H}_9 + \text{CH}_3\text{OH}$	11.78	0	7.00	10.39	0	9.18
198.	$\text{pC}_4\text{H}_9$	$= \text{C}_2\text{H}_5 + \text{C}_2\text{H}_4$	13.40	0	28.80	11.48	0	8.00
199.	$\text{pC}_4\text{H}_9$	$= \text{1C}_4\text{H}_8 + \text{H}$	13.10	0	38.60	13.00	0	1.50
200.	$\text{pC}_4\text{H}_9 + \text{O}_2$	$= \text{1C}_4\text{H}_8 + \text{HO}_2$	12.00	0	2.00	11.29	0	15.85
201.	$\text{sC}_4\text{H}_9$	$= \text{2C}_4\text{H}_8 + \text{H}$	12.70	0	37.90	13.00	0	1.50
202.	$\text{sC}_4\text{H}_9$	$= \text{1C}_4\text{H}_8 + \text{H}$	13.30	0	40.40	13.00	0	1.50
203.	$\text{sC}_4\text{H}_9$	$= \text{C}_3\text{H}_6 + \text{CH}_3$	14.30	0	33.20	11.50	0	7.40
204.	$\text{sC}_4\text{H}_9 + \text{O}_2$	$= \text{1C}_4\text{H}_8 + \text{HO}_2$	12.00	0	4.50	11.29	0	18.35
205.	$\text{sC}_4\text{H}_9 + \text{O}_2$	$= \text{2C}_4\text{H}_8 + \text{HO}_2$	12.30	0	4.25	11.59	0	18.10
206.	$\text{1C}_4\text{H}_8$	$= \text{C}_4\text{H}_7 + \text{H}$	18.61	-1	97.35	13.70	0	0.00
207.	$\text{2C}_4\text{H}_8$	$= \text{C}_4\text{H}_7 + \text{H}$	18.61	-1	97.35	13.70	0	0.00
208.	$\text{1C}_4\text{H}_8 + \text{H}$	$= \text{C}_4\text{H}_7 + \text{H}_2$	13.70	0	3.90	12.00	0	13.99
209.	$\text{2C}_4\text{H}_8 + \text{H}$	$= \text{C}_4\text{H}_7 + \text{H}_2$	13.70	0	3.80	12.00	0	13.89
210.	$\text{1C}_4\text{H}_8 + \text{OH}$	$= \text{C}_4\text{H}_7 + \text{H}_2\text{O}$	13.15	0	3.06	13.15	0	28.30
211.	$\text{2C}_4\text{H}_8 + \text{OH}$	$= \text{C}_4\text{H}_7 + \text{H}_2\text{O}$	13.36	0	3.06	13.36	0	28.30
212.	$\text{1C}_4\text{H}_8 + \text{CH}_3$	$= \text{C}_4\text{H}_7 + \text{CH}_4$	11.00	0	7.30	11.78	0	17.86
213.	$\text{2C}_4\text{H}_8 + \text{CH}_3$	$= \text{C}_4\text{H}_7 + \text{CH}_4$	11.00	0	8.20	11.78	0	18.76
214.	$\text{1C}_4\text{H}_8 + \text{O}$	$= \text{C}_3\text{H}_6 + \text{CH}_2\text{O}$	12.70	0	0.00	12.14	0	81.33
215.	$\text{2C}_4\text{H}_8 + \text{O}$	$= \text{iC}_3\text{H}_7 + \text{HCO}$	12.78	0	0.00	11.35	0	25.81
216.	$\text{2C}_4\text{H}_8 + \text{O}$	$= \text{C}_2\text{H}_4 + \text{CH}_3\text{CHO}$	12.00	0	0.00	11.20	0	84.25
217.	$\text{1C}_4\text{H}_8 + \text{OH}$	$= \text{nC}_3\text{H}_7 + \text{CH}_2\text{O}$	12.18	0	0.00	12.21	0	13.23
218.	$\text{2C}_4\text{H}_8 + \text{OH}$	$= \text{C}_2\text{H}_5 + \text{CH}_3\text{CHO}$	12.48	0	0.00	12.46	0	19.93
219.	$\text{C}_4\text{H}_7$	$= \text{C}_4\text{H}_6 + \text{H}$	14.08	0	49.30	13.60	0	1.30
220.	$\text{C}_4\text{H}_7$	$= \text{C}_2\text{H}_4 + \text{C}_2\text{H}_3$	11.00	0	37.00	10.70	0	7.00
221.	$\text{C}_4\text{H}_7 + \text{O}_2$	$= \text{C}_4\text{H}_6 + \text{HO}_2$	11.00	0	0.00	11.00	0	17.00
222.	$\text{C}_4\text{H}_7 + \text{H}$	$= \text{C}_4\text{H}_6 + \text{H}_2$	13.50	0	0.00	13.03	0	56.81
223.	$\text{C}_4\text{H}_7 + \text{C}_2\text{H}_3$	$= \text{C}_4\text{H}_6 + \text{C}_2\text{H}_4$	12.60	0	0.00	13.06	0	57.71
224.	$\text{C}_4\text{H}_7 + \text{C}_2\text{H}_5$	$= \text{C}_4\text{H}_6 + \text{C}_2\text{H}_6$	12.60	0	0.00	12.51	0	49.84
225.	$\text{C}_4\text{H}_7 + \text{C}_2\text{H}_5$	$= \text{1C}_4\text{H}_8 + \text{C}_2\text{H}_4$	11.70	0	0.00	11.93	0	56.33
226.	$\text{C}_4\text{H}_7 + \text{C}_2\text{H}_5$	$= \text{2C}_4\text{H}_8 + \text{C}_2\text{H}_4$	11.70	0	0.00	11.93	0	56.33
227.	$\text{C}_4\text{H}_7 + \text{C}_3\text{H}_5$	$= \text{C}_4\text{H}_6 + \text{C}_3\text{H}_6$	12.80	0	0.00	10.00	0	50.00
228.	$\text{C}_4\text{H}_6$	$= \text{C}_2\text{H}_3 + \text{C}_2\text{H}_3$	19.60	-1	98.15	13.10	0	0.00
229.	$\text{C}_4\text{H}_6 + \text{OH}$	$= \text{C}_2\text{H}_5 + \text{CH}_2\text{CO}$	12.00	0	0.00	12.57	0	30.02
230.	$\text{C}_4\text{H}_6 + \text{OH}$	$= \text{C}_3\text{H}_5 + \text{CH}_2\text{O}$	12.00	0	0.00	6.54	0	71.06
231.	$\text{C}_4\text{H}_6 + \text{OH}$	$= \text{C}_2\text{H}_3 + \text{CH}_3\text{CHO}$	12.00	0	0.00	11.74	0	18.55
232.	$\text{C}_4\text{H}_6 + \text{O}$	$= \text{C}_2\text{H}_4 + \text{CH}_2\text{CO}$	12.00	0	0.00	11.80	0	94.34
233.	$\text{C}_4\text{H}_6 + \text{O}$	$= \text{C}_3\text{H}_4 + \text{CH}_2\text{O}$	12.00	0	0.00	12.03	0	79.05
234.	$\text{C}_2\text{H}_3 + \text{C}_2\text{H}_4$	$= \text{C}_4\text{H}_6 + \text{H}$	11.70	0	7.30	13.00	0	4.70
235.	$\text{C}_5\text{H}_{10}$	$= \text{CH}_3 + \text{C}_4\text{H}_7$	19.00	-1	81.55	13.40	0	0.00
236.	$\text{C}_5\text{H}_{10} + \text{O}$	$= \text{1C}_4\text{H}_8 + \text{CH}_2\text{O}$	12.93	0	0.00	12.34	0	85.43
237.	$\text{C}_5\text{H}_{10} + \text{O}$	$= \text{C}_3\text{H}_6 + \text{CH}_3\text{CHO}$	12.93	0	0.00	11.55	0	88.01
238.	$\text{C}_5\text{H}_{10} + \text{OH}$	$= \text{pC}_4\text{H}_9 + \text{CH}_2\text{O}$	12.00	0	0.00	12.01	0	50.00
239.	$\text{C}_5\text{H}_{10} + \text{OH}$	$= \text{nC}_3\text{H}_7 + \text{CH}_3\text{CHO}$	12.00	0	0.00	11.22	0	50.00
240.	$\text{C}_2\text{H}_5 + \text{H}$	$= \text{CH}_3 + \text{CH}_3$	13.50	0	0.00	10.70	0	7.40

Table I (continued)  
Fuel oxidation mechanism. Reaction rates in  
cm<sup>3</sup>-mole-sec-kcal units,  $k = AT^n \exp(-E_a/RT)$

<u>Reaction</u>			Forward rate			Reverse rate		
			<u>log A</u>	<u>n</u>	<u>E<sub>a</sub></u>	<u>log A</u>	<u>n</u>	<u>E<sub>a</sub></u>
241.	CH <sub>3</sub> OH+O <sub>2</sub>	= CH <sub>2</sub> OH+HO <sub>2</sub>	13.60	0	50.90	7.17	1.66	1.35
242.	C <sub>2</sub> H <sub>4</sub> +O <sub>2</sub>	= C <sub>2</sub> H <sub>3</sub> +HO <sub>2</sub>	13.60	0	61.50	12.00	0	0.00
243.	C <sub>2</sub> H <sub>4</sub> +CH <sub>3</sub>	= C <sub>2</sub> H <sub>3</sub> +CH <sub>4</sub>	13.00	0	13.00	13.48	0	12.58
244.	C <sub>3</sub> H <sub>6</sub> +O <sub>2</sub>	= C <sub>3</sub> H <sub>5</sub> +HO <sub>2</sub>	14.00	0	39.00	11.00	0	0.00

All third body efficiencies are 1.0, except for the following:

$k_6(\text{H}_2\text{O}) = 20k_6(\text{N}_2)$

$k_7(\text{H}_2\text{O}) = 21k_7(\text{N}_2)$ ;  $k_7(\text{CO}_2) = 5k_7(\text{N}_2)$ ;  $k_7(\text{CO}) = 2k_7(\text{N}_2)$ ;  $k_7(\text{H}_2) = 3.3k_7(\text{N}_2)$

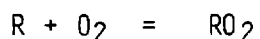
$k_{13}(\text{H}_2\text{O}) = 6k_{13}(\text{N}_2)$ ;  $k_{13}(\text{O}_2) = 0.78k_{13}(\text{N}_2)$ ;  $k_{13}(\text{H}_2\text{O}_2) = 6.6k_{13}(\text{N}_2)$

$k_{17}(\text{H}_2\text{O}) = 6k_{17}(\text{N}_2)$ ;  $k_{17}(\text{H}) = 2k_{17}(\text{N}_2)$ ;  $k_{17}(\text{H}_2) = 3k_{17}(\text{N}_2)$

branched chain iso-butane, which has a higher Research octane rating of 102 [18]. Future numerical modeling work will examine the role that molecular structure has on autoignition, as well as extension to even larger straight chain hydrocarbon fuel molecules.

During the engine cycle, the end gas, the last portion of fuel-air mixture in the combustion chamber to be consumed, is subjected to temperatures in the range of 450 to 900 K for a considerable length of time (as long as 40 ms at 600 rpm in the low compression engine to be discussed later). Downs, Walsh, and Wheeler [19] showed that "cool flame" processes occur at these temperatures and produce peroxides that may act as pro-knock agents. In order to consider additional kinetic paths which occur below 1000 K, another kinetic submechanism (Table II) was added to the high temperature mechanism. This submechanism contains chemical kinetic steps which pertain primarily to the formation and consumption of alkyl hydroperoxides. Much of the submechanism was taken from a concurrent study on the low temperature oxidation of acetaldehyde [20], and additional rate parameters were estimated on the basis of the work of Benson [21].

At lower temperatures, addition reactions, including particularly



where R is a hydrocarbon radical species, dominate over the direct radical oxidation and decomposition steps, leading to degenerate branching, a negative temperature coefficient regime, and multi-stage ignition. The present combined mechanism correctly predicts this type of behavior, reproducing experimental results from static reactors [20,22] and in rapid compression experiments [23] for acetaldehyde oxidation. Further applications of the model to simulate cool-flame and other low temperature combustion of other fuels are in progress, and the principal features of

Table II

Low temperature kinetics submechanism. Reaction rates  
in cm<sup>3</sup>-mole-sec-kcal units,  $k = AT^n \exp(E_a/RT)$

Reaction			Forward rate			Reverse rate		
			log A	n	E <sub>a</sub>	log A	n	E <sub>a</sub>
1.	CH <sub>3</sub> O <sub>2</sub>	= CH <sub>3</sub> +O <sub>2</sub>	13.31	0	27.63	12.00	0	0.00
2.	C <sub>2</sub> H <sub>5</sub> O <sub>2</sub>	= C <sub>2</sub> H <sub>5</sub> +O <sub>2</sub>	13.81	0	27.63	12.00	0	0.00
3.	nC <sub>3</sub> H <sub>7</sub> O <sub>2</sub>	= nC <sub>3</sub> H <sub>7</sub> +O <sub>2</sub>	13.81	0	27.63	12.00	0	0.00
4.	iC <sub>3</sub> H <sub>7</sub> O <sub>2</sub>	= iC <sub>3</sub> H <sub>7</sub> +O <sub>2</sub>	13.81	0	27.63	12.00	0	0.00
5.	pC <sub>4</sub> H <sub>9</sub> O <sub>2</sub>	= pC <sub>4</sub> H <sub>9</sub> +O <sub>2</sub>	13.81	0	27.63	12.00	0	0.00
6.	sC <sub>4</sub> H <sub>9</sub> O <sub>2</sub>	= sC <sub>4</sub> H <sub>9</sub> +O <sub>2</sub>	13.81	0	27.63	12.00	0	0.00
7.	CH <sub>3</sub> O <sub>2</sub> +C <sub>3</sub> H <sub>8</sub>	= CH <sub>3</sub> O <sub>2</sub> H+nC <sub>3</sub> H <sub>7</sub>	11.51	0	16.50	10.41	0	8.00
8.	CH <sub>3</sub> O <sub>2</sub> +C <sub>3</sub> H <sub>8</sub>	= CH <sub>3</sub> O <sub>2</sub> H+iC <sub>3</sub> H <sub>7</sub>	11.51	0	16.50	10.41	0	8.00
9.	CH <sub>3</sub> O <sub>2</sub> +C <sub>4</sub> H <sub>10</sub>	= CH <sub>3</sub> O <sub>2</sub> H+pC <sub>4</sub> H <sub>9</sub>	11.51	0	16.50	10.41	0	8.00
10.	CH <sub>3</sub> O <sub>2</sub> +C <sub>4</sub> H <sub>10</sub>	= CH <sub>3</sub> O <sub>2</sub> H+sC <sub>4</sub> H <sub>9</sub>	11.81	0	16.50	10.72	0	8.00
11.	C <sub>2</sub> H <sub>5</sub> O <sub>2</sub> +C <sub>3</sub> H <sub>8</sub>	= C <sub>2</sub> H <sub>5</sub> O <sub>2</sub> H+nC <sub>3</sub> H <sub>7</sub>	11.51	0	16.50	10.41	0	8.00
12.	C <sub>2</sub> H <sub>5</sub> O <sub>2</sub> +C <sub>3</sub> H <sub>8</sub>	= C <sub>2</sub> H <sub>5</sub> O <sub>2</sub> H+iC <sub>3</sub> H <sub>7</sub>	11.51	0	16.50	10.41	0	8.00
13.	C <sub>2</sub> H <sub>5</sub> O <sub>2</sub> +C <sub>4</sub> H <sub>10</sub>	= C <sub>2</sub> H <sub>5</sub> O <sub>2</sub> H+pC <sub>4</sub> H <sub>9</sub>	11.51	0	16.50	10.41	0	8.00
14.	C <sub>2</sub> H <sub>5</sub> O <sub>2</sub> +C <sub>4</sub> H <sub>10</sub>	= C <sub>2</sub> H <sub>5</sub> O <sub>2</sub> H+sC <sub>4</sub> H <sub>9</sub>	11.81	0	16.50	10.72	0	8.00
15.	nC <sub>3</sub> H <sub>7</sub> O <sub>2</sub> +C <sub>3</sub> H <sub>8</sub>	= nC <sub>3</sub> H <sub>7</sub> O <sub>2</sub> H+nC <sub>3</sub> H <sub>7</sub>	11.51	0	16.50	10.41	0	8.00
16.	nC <sub>3</sub> H <sub>7</sub> O <sub>2</sub> +C <sub>3</sub> H <sub>8</sub>	= nC <sub>3</sub> H <sub>7</sub> O <sub>2</sub> H+iC <sub>3</sub> H <sub>7</sub>	11.51	0	16.50	10.41	0	8.00
17.	nC <sub>3</sub> H <sub>7</sub> O <sub>2</sub> +C <sub>4</sub> H <sub>10</sub>	= nC <sub>3</sub> H <sub>7</sub> O <sub>2</sub> H+pC <sub>4</sub> H <sub>9</sub>	11.51	0	16.50	10.41	0	8.00
18.	nC <sub>3</sub> H <sub>7</sub> O <sub>2</sub> +C <sub>4</sub> H <sub>10</sub>	= nC <sub>3</sub> H <sub>7</sub> O <sub>2</sub> H+sC <sub>4</sub> H <sub>9</sub>	11.81	0	16.50	10.72	0	8.00
19.	iC <sub>3</sub> H <sub>7</sub> O <sub>2</sub> +C <sub>3</sub> H <sub>8</sub>	= iC <sub>3</sub> H <sub>7</sub> O <sub>2</sub> H+nC <sub>3</sub> H <sub>7</sub>	11.51	0	16.50	10.41	0	8.00
20.	iC <sub>3</sub> H <sub>7</sub> O <sub>2</sub> +C <sub>3</sub> H <sub>8</sub>	= iC <sub>3</sub> H <sub>7</sub> O <sub>2</sub> H+iC <sub>3</sub> H <sub>7</sub>	11.51	0	16.50	10.41	0	8.00
21.	iC <sub>3</sub> H <sub>7</sub> O <sub>2</sub> +C <sub>4</sub> H <sub>10</sub>	= iC <sub>3</sub> H <sub>7</sub> O <sub>2</sub> H+pC <sub>4</sub> H <sub>9</sub>	11.51	0	16.50	10.41	0	8.00
22.	iC <sub>3</sub> H <sub>7</sub> O <sub>2</sub> +C <sub>4</sub> H <sub>10</sub>	= iC <sub>3</sub> H <sub>7</sub> O <sub>2</sub> H+sC <sub>4</sub> H <sub>9</sub>	11.81	0	16.50	10.72	0	8.00
23.	pC <sub>4</sub> H <sub>9</sub> O <sub>2</sub> +C <sub>3</sub> H <sub>8</sub>	= pC <sub>4</sub> H <sub>9</sub> O <sub>2</sub> H+nC <sub>3</sub> H <sub>7</sub>	11.51	0	16.50	10.41	0	8.00
24.	pC <sub>4</sub> H <sub>9</sub> O <sub>2</sub> +C <sub>3</sub> H <sub>8</sub>	= pC <sub>4</sub> H <sub>9</sub> O <sub>2</sub> H+iC <sub>3</sub> H <sub>7</sub>	11.51	0	16.50	10.41	0	8.00
25.	pC <sub>4</sub> H <sub>9</sub> O <sub>2</sub> +C <sub>4</sub> H <sub>10</sub>	= pC <sub>4</sub> H <sub>9</sub> O <sub>2</sub> H+pC <sub>4</sub> H <sub>9</sub>	11.51	0	16.50	10.41	0	8.00
26.	pC <sub>4</sub> H <sub>9</sub> O <sub>2</sub> +C <sub>4</sub> H <sub>10</sub>	= pC <sub>4</sub> H <sub>9</sub> O <sub>2</sub> H+sC <sub>4</sub> H <sub>9</sub>	11.81	0	16.50	10.72	0	8.00
27.	sC <sub>4</sub> H <sub>9</sub> O <sub>2</sub> +C <sub>3</sub> H <sub>8</sub>	= sC <sub>4</sub> H <sub>9</sub> O <sub>2</sub> H+nC <sub>3</sub> H <sub>7</sub>	11.51	0	16.50	10.41	0	8.00
28.	sC <sub>4</sub> H <sub>9</sub> O <sub>2</sub> +C <sub>3</sub> H <sub>8</sub>	= sC <sub>4</sub> H <sub>9</sub> O <sub>2</sub> H+iC <sub>3</sub> H <sub>7</sub>	11.51	0	16.50	10.41	0	8.00
29.	sC <sub>4</sub> H <sub>9</sub> O <sub>2</sub> +C <sub>4</sub> H <sub>10</sub>	= sC <sub>4</sub> H <sub>9</sub> O <sub>2</sub> H+pC <sub>4</sub> H <sub>9</sub>	11.51	0	16.50	10.41	0	8.00
30.	sC <sub>4</sub> H <sub>9</sub> O <sub>2</sub> +C <sub>4</sub> H <sub>10</sub>	= sC <sub>4</sub> H <sub>9</sub> O <sub>2</sub> H+sC <sub>4</sub> H <sub>9</sub>	11.81	0	16.50	10.72	0	8.00
31.	CH <sub>3</sub> O <sub>2</sub> +CH <sub>2</sub> O	= CH <sub>3</sub> O <sub>2</sub> H+HCO	11.11	0	9.00	10.40	0	10.10
32.	CH <sub>3</sub> O <sub>2</sub> +CH <sub>3</sub> CHO	= CH <sub>3</sub> O <sub>2</sub> H+CH <sub>3</sub> CO	11.32	0	9.53	9.70	0	10.10
33.	C <sub>2</sub> H <sub>5</sub> O <sub>2</sub> +CH <sub>2</sub> O	= C <sub>2</sub> H <sub>5</sub> O <sub>2</sub> H+HCO	11.11	0	9.00	10.40	0	10.10
34.	C <sub>2</sub> H <sub>5</sub> O <sub>2</sub> +CH <sub>3</sub> CHO	= C <sub>2</sub> H <sub>5</sub> O <sub>2</sub> H+CH <sub>3</sub> CO	11.32	0	9.53	9.70	0	10.10
35.	nC <sub>3</sub> H <sub>7</sub> O <sub>2</sub> +CH <sub>2</sub> O	= nC <sub>3</sub> H <sub>7</sub> O <sub>2</sub> H+HCO	11.11	0	9.00	10.40	0	10.10
36.	nC <sub>3</sub> H <sub>7</sub> O <sub>2</sub> +CH <sub>3</sub> CHO	= nC <sub>3</sub> H <sub>7</sub> O <sub>2</sub> H+CH <sub>3</sub> CO	12.78	0	12.00	10.40	0	10.10
37.	iC <sub>3</sub> H <sub>7</sub> O <sub>2</sub> +CH <sub>2</sub> O	= iC <sub>3</sub> H <sub>7</sub> O <sub>2</sub> H+HCO	11.11	0	9.00	10.40	0	10.10
38.	iC <sub>3</sub> H <sub>7</sub> O <sub>2</sub> +CH <sub>3</sub> CHO	= iC <sub>3</sub> H <sub>7</sub> O <sub>2</sub> H+CH <sub>3</sub> CO	12.78	0	12.00	10.40	0	10.10
39.	pC <sub>4</sub> H <sub>9</sub> O <sub>2</sub> +CH <sub>2</sub> O	= pC <sub>4</sub> H <sub>9</sub> O <sub>2</sub> H+HCO	11.11	0	9.00	10.40	0	10.10
40.	pC <sub>4</sub> H <sub>9</sub> O <sub>2</sub> +CH <sub>3</sub> CHO	= pC <sub>4</sub> H <sub>9</sub> O <sub>2</sub> H+CH <sub>3</sub> CO	12.78	0	12.00	10.40	0	10.10
41.	sC <sub>4</sub> H <sub>9</sub> O <sub>2</sub> +CH <sub>2</sub> O	= sC <sub>4</sub> H <sub>9</sub> O <sub>2</sub> H+HCO	11.11	0	9.00	10.40	0	10.10
42.	sC <sub>4</sub> H <sub>9</sub> O <sub>2</sub> +CH <sub>3</sub> CHO	= sC <sub>4</sub> H <sub>9</sub> O <sub>2</sub> H+CH <sub>3</sub> CO	12.78	0	12.00	10.40	0	10.10
43.	CH <sub>3</sub> O <sub>2</sub> +HO <sub>2</sub>	= CH <sub>3</sub> O <sub>2</sub> H+O <sub>2</sub>	10.66	0	-2.60	12.48	0	39.00
44.	CH <sub>3</sub> O <sub>2</sub> +HO <sub>2</sub>	= CH <sub>3</sub> O+OH+O <sub>2</sub>	12.00	0	0.00	*		
45.	C <sub>2</sub> H <sub>5</sub> O <sub>2</sub> +HO <sub>2</sub>	= C <sub>2</sub> H <sub>5</sub> O <sub>2</sub> H+O <sub>2</sub>	10.66	0	-2.60	12.48	0	39.00

Table II (continued)

Low temperature kinetics submechanism. Reaction rates  
in cm<sup>3</sup>-mole-sec-kcal units,  $k = AT^n \exp(E_a/RT)$

Reaction			Forward rate			Reverse rate		
			log A	n	E <sub>a</sub>	log A	n	E <sub>a</sub>
46.	nC <sub>3</sub> H <sub>7</sub> O <sub>2</sub> +HO <sub>2</sub>	= nC <sub>3</sub> H <sub>7</sub> O <sub>2</sub> H+O <sub>2</sub>	10.66	0	-2.60	12.48	0	39.00
47.	iC <sub>3</sub> H <sub>7</sub> O <sub>2</sub> +HO <sub>2</sub>	= iC <sub>3</sub> H <sub>7</sub> O <sub>2</sub> H+O <sub>2</sub>	10.66	0	-2.60	12.48	0	39.00
48.	pC <sub>4</sub> H <sub>9</sub> O <sub>2</sub> +HO <sub>2</sub>	= pC <sub>4</sub> H <sub>9</sub> O <sub>2</sub> H+O <sub>2</sub>	10.66	0	-2.60	12.48	0	39.00
49.	sC <sub>4</sub> H <sub>9</sub> O <sub>2</sub> +HO <sub>2</sub>	= sC <sub>4</sub> H <sub>9</sub> O <sub>2</sub> H+O <sub>2</sub>	10.66	0	-2.60	12.48	0	39.00
50.	CH <sub>3</sub> O <sub>2</sub> +CH <sub>3</sub> O <sub>2</sub>	= CH <sub>3</sub> O+CH <sub>3</sub> O+O <sub>2</sub>	12.57	0	2.20	*		
51.	CH <sub>3</sub> O <sub>2</sub> +CH <sub>3</sub> O <sub>2</sub>	= CH <sub>2</sub> O+CH <sub>3</sub> OH+O <sub>2</sub>	11.26	0	0.00	*		
52.	CH <sub>3</sub> O <sub>2</sub> CH <sub>3</sub> +O <sub>2</sub>	= CH <sub>3</sub> O <sub>2</sub> +CH <sub>3</sub> O <sub>2</sub>	0.00	0	0.00	11.70	0	2.00
53.	CH <sub>3</sub> O <sub>2</sub> CH <sub>3</sub>	= CH <sub>3</sub> O+CH <sub>3</sub> O	15.48	0	37.00	*		
54.	CH <sub>3</sub> O <sub>2</sub> +CH <sub>3</sub>	= CH <sub>3</sub> O+CH <sub>3</sub> O	13.56	0	0.00	10.30	0	0.00
55.	CH <sub>3</sub> O <sub>2</sub> H	= CH <sub>3</sub> O+OH	14.92	0	43.00	11.00	0	0.00
56.	C <sub>2</sub> H <sub>5</sub> O <sub>2</sub> H	= C <sub>2</sub> H <sub>5</sub> O+OH	14.92	0	43.00	11.00	0	0.00
57.	nC <sub>3</sub> H <sub>7</sub> O <sub>2</sub> H	= nC <sub>3</sub> H <sub>7</sub> O+OH	14.92	0	43.00	11.00	0	0.00
58.	iC <sub>3</sub> H <sub>7</sub> O <sub>2</sub> H	= iC <sub>3</sub> H <sub>7</sub> O+OH	14.92	0	43.00	11.00	0	0.00
59.	pC <sub>4</sub> H <sub>9</sub> O <sub>2</sub> H	= pC <sub>4</sub> H <sub>9</sub> O+OH	14.92	0	43.00	11.00	0	0.00
60.	sC <sub>4</sub> H <sub>9</sub> O <sub>2</sub> H	= sC <sub>4</sub> H <sub>9</sub> O+OH	14.92	0	43.00	11.00	0	0.00
61.	OH+CH <sub>3</sub> O <sub>2</sub> H	= CH <sub>3</sub> O <sub>2</sub> +H <sub>2</sub> O	13.25	0	1.00	13.23	0	32.80
62.	C <sub>2</sub> H <sub>5</sub> O	= CH <sub>3</sub> +CH <sub>2</sub> O	15.00	0	21.60	7.00	1	13.60
63.	nC <sub>3</sub> H <sub>7</sub> O	= C <sub>2</sub> H <sub>5</sub> +CH <sub>2</sub> O	13.23	0	17.82	5.30	1	9.82
64.	iC <sub>3</sub> H <sub>7</sub> O	= CH <sub>3</sub> +CH <sub>3</sub> CHO	13.18	0	14.82	5.30	1	9.82
65.	pC <sub>4</sub> H <sub>9</sub> O	= nC <sub>3</sub> H <sub>7</sub> +CH <sub>2</sub> O	13.23	0	17.82	5.30	1	9.82
66.	sC <sub>4</sub> H <sub>9</sub> O	= C <sub>2</sub> H <sub>5</sub> +CH <sub>3</sub> CHO	13.18	0	14.82	5.30	1	9.82
67.	C <sub>2</sub> H <sub>5</sub> O+O <sub>2</sub>	= CH <sub>3</sub> CHO+HO <sub>2</sub>	12.50	0	4.00	11.81	0	30.17
68.	CH <sub>3</sub> O+CH <sub>3</sub> CHO	= CH <sub>3</sub> OH+CH <sub>3</sub> CO	11.78	0	3.30	11.48	0	18.20
69.	CH <sub>3</sub> O+CH <sub>3</sub> OH	= CH <sub>2</sub> OH+CH <sub>3</sub> OH	11.30	0	7.00	4.34	1.66	10.85
70.	CH <sub>3</sub> CO <sub>3</sub>	= CH <sub>3</sub> CO+O <sub>2</sub>	17.78	-1	40.00	12.00	0	0.00
71.	CH <sub>3</sub> CO <sub>3</sub> +C <sub>4</sub> H <sub>10</sub>	= CH <sub>3</sub> CO <sub>3</sub> H+pC <sub>4</sub> H <sub>9</sub>	11.51	0	16.50	10.41	0	8.00
72.	CH <sub>3</sub> CO <sub>3</sub> +C <sub>4</sub> H <sub>10</sub>	= CH <sub>3</sub> CO <sub>3</sub> H+sC <sub>4</sub> H <sub>9</sub>	11.81	0	16.50	10.72	0	8.00
73.	CH <sub>3</sub> CO <sub>3</sub> +CH <sub>3</sub> CHO	= CH <sub>3</sub> CO <sub>3</sub> H+CH <sub>3</sub> CO	12.00	0	7.58	10.30	0	10.00
74.	CH <sub>3</sub> CO <sub>3</sub> +HO <sub>2</sub>	= CH <sub>3</sub> CO <sub>3</sub> H+O <sub>2</sub>	12.00	0	0.00	13.60	0	51.00
75.	CH <sub>3</sub> CO <sub>3</sub> +HO <sub>2</sub>	= CH <sub>3</sub> CO <sub>2</sub> +OH+O <sub>2</sub>	12.00	0	0.00	*		
76.	CH <sub>3</sub> CO <sub>3</sub> +CH <sub>3</sub> CO <sub>3</sub>	= CH <sub>3</sub> CO <sub>2</sub> +CH <sub>3</sub> O <sub>2</sub> +O <sub>2</sub>	12.26	0	0.00	*		
77.	CH <sub>3</sub> CO <sub>3</sub> H	= CH <sub>3</sub> CO <sub>2</sub> +OH	15.60	0	40.00	*		
78.	CH <sub>3</sub> CO <sub>3</sub> H	= CH <sub>3</sub> +CO <sub>2</sub> +OH	14.30	0	40.15	*		
79.	CH <sub>3</sub> CO <sub>2</sub>	= CH <sub>3</sub> +CO <sub>2</sub>	15.64	0	10.50	*		
80.	CH <sub>3</sub> CO <sub>3</sub> +CH <sub>3</sub> O <sub>2</sub>	= CH <sub>3</sub> CO <sub>2</sub> H+CH <sub>2</sub> O+O <sub>2</sub>	11.48	0	0.00	*		
81.	CH <sub>3</sub> CO <sub>3</sub> +CH <sub>3</sub> O <sub>2</sub>	= CH <sub>3</sub> CO <sub>2</sub> +CH <sub>3</sub> O+O <sub>2</sub>	12.26	0	0.00	*		
82.	CH <sub>3</sub> OH+OH	= CH <sub>3</sub> O+H <sub>2</sub> O	13.09	0	3.25	13.50	0	21.46

\* No reverse rate included

these low temperature mechanisms have been incorporated into the submechanism in Table II. The overall adequacy of the combined mechanism of Table I and II is supported by successful comparisons between computed species concentrations and experimental data obtained for n-butane oxidation in an engine by gas sampling techniques by Cernansky et al. [24]. Additionally, Leppard [25] used the present combined mechanism to model autoignition in a Cooperative Fuels Research (CFR) engine. With his zero-dimensional model of the end gas, he examined autoignition at two engine speeds (600 and 1600 rpm) and three equivalence ratios (0.8, 1.0, and 1.2) for propane and n-butane. In preliminary results, he obtained good agreement between measured and predicted autoignition times.

## RESULTS

Autoignition calculations were performed with the objective of identifying the primary chemical reactions that can lead to engine knock and the relevant time scales involved. These calculations attempt to simulate the conditions to which end gas in an actual engine is subjected prior to knock. Three types of calculations were used to characterize autoignition in a stoichiometric mixture of n-butane/air, and each type had advantages in its treatment of the problem. In the first set of calculations, a sample of fuel-air mixture was constrained to follow temperatures and pressures measured in the end gas of a spark ignition engine by Green and Smith [16,17]. By following the measured temperatures, this treatment accounted for heat transfer between the end gas and the combustion chamber walls. These calculations were started at 23 degrees before top dead center (TDC) which was the time of the first available temperature measurement point. In the second type of calculation, only the



pressure histories measured by Green and Smith were followed. As a result, a larger portion of the engine cycle was covered by starting at bottom dead center. This calculation included the early part of the compression stroke when the end gas was at reduced temperatures (500 K to 700 K) and low temperature kinetics may have been important. Experimental data for these extended times were available for the pressure but not for the temperature so that an assumption of adiabatic compression of the end gas was necessary. In the third and most simplified treatment, the calculations did not follow the measured temperatures or pressures. Alternatively, constant volume, adiabatic combustion was assumed. Calculations are performed over a range of initial temperatures (600-1000 K) and at an initial pressure of 30 atm which is typical of the pressure that the end gas is subjected to just prior to knock. With the appropriate choice of initial temperature, this approach showed trends very similar to the two previous sets of calculations in which the temperature and pressure varied due to the piston stroke and due to compression by the flame.

Typical results were obtained for each type of calculation and are presented in the following section. All of these computations used the combined kinetic mechanism of Tables I and II over the entire temperature range considered. Each series of calculations included a sensitivity study which identified the primary reactions that control autoignition.

#### 1. Calculations following measured temperature and pressure.

A series of calculations followed reactions taking place in a sample of n-butane/air subjected to measured temperature and pressure histories. Green and Smith [16,17] experimentally measured these temperatures and pressures in the end gas of a spark-ignition engine that could be operated

in a highly reproducible, knocking condition. Each calculation was started at 23 degrees (6 ms) before TDC, the time of the first experimental temperature data point. A curve fit to the measured pressures is shown in Fig. 1a and was followed for the entire calculation. These pressures were measured when the engine was operating very close to the knock point, but it was not quite knocking. The pressure history when the engine was knocking was not used in the calculation, since the sharp rise in the measured pressure trace when knock occurred might induce autoignition in the calculation. The portion of the experimental pressure curve prior to the knock point was very similar for both the knocking and non-knocking case, with a difference of only 0.24 atm in initial pressure between the two cases [17]. The measured temperatures were followed until the time of the last temperature data point which was taken just before autoignition occurred in the engine. By following the measured temperatures, any heat transfer between the end gas and its surroundings along with any heat release that might have occurred in the actual end gas was incorporated in the calculation.

After the final temperature data point, the measured temperatures were no longer followed, and the reacting mixture was assumed to burn adiabatically. The volume of the reacting mixture was adjusted to match the measured pressure data. This adjustment in volume accounted for both the motion of the piston and the compression by the burnt products behind the propagating flame front in the combustion chamber. The calculated time of autoignition was defined by the steep temperature rise which occurs at autoignition.

The temperature, pressure, and fuel concentration histories are shown in Fig. 1a and 1b. The autoignition time is predicted to be 3.6 ms after

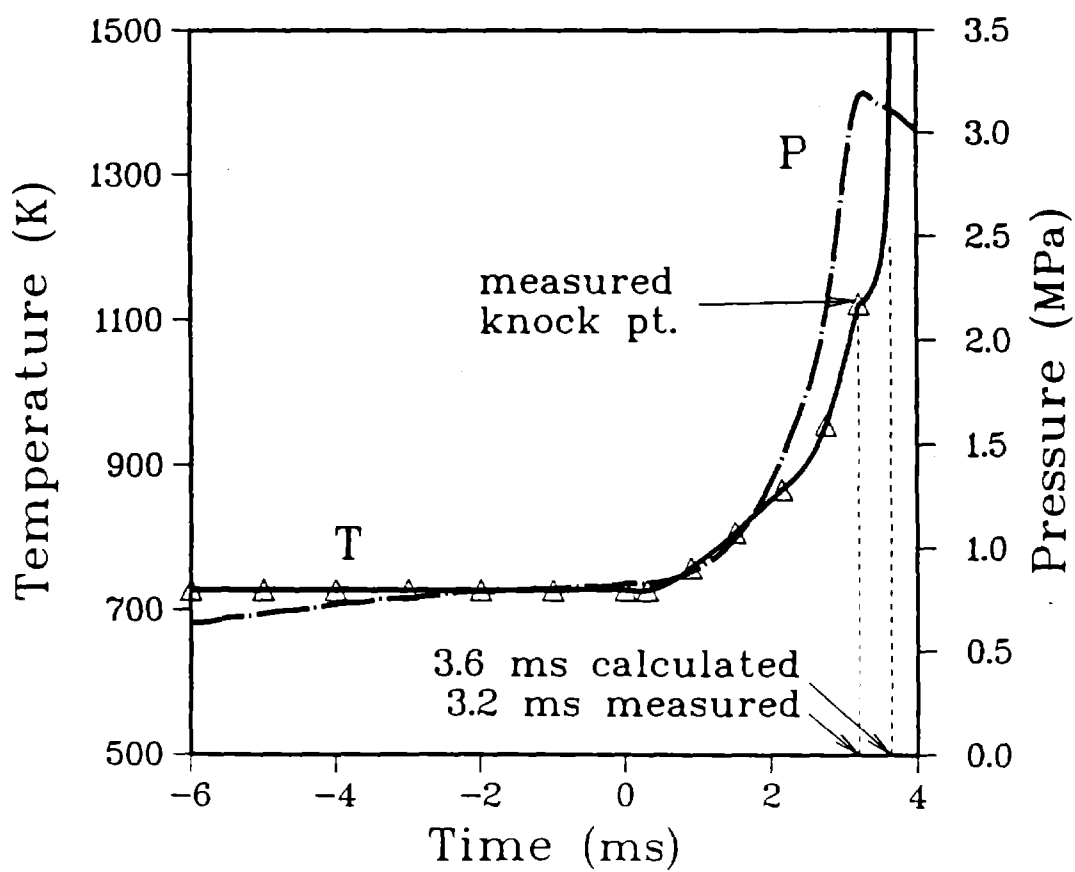


Figure 1a

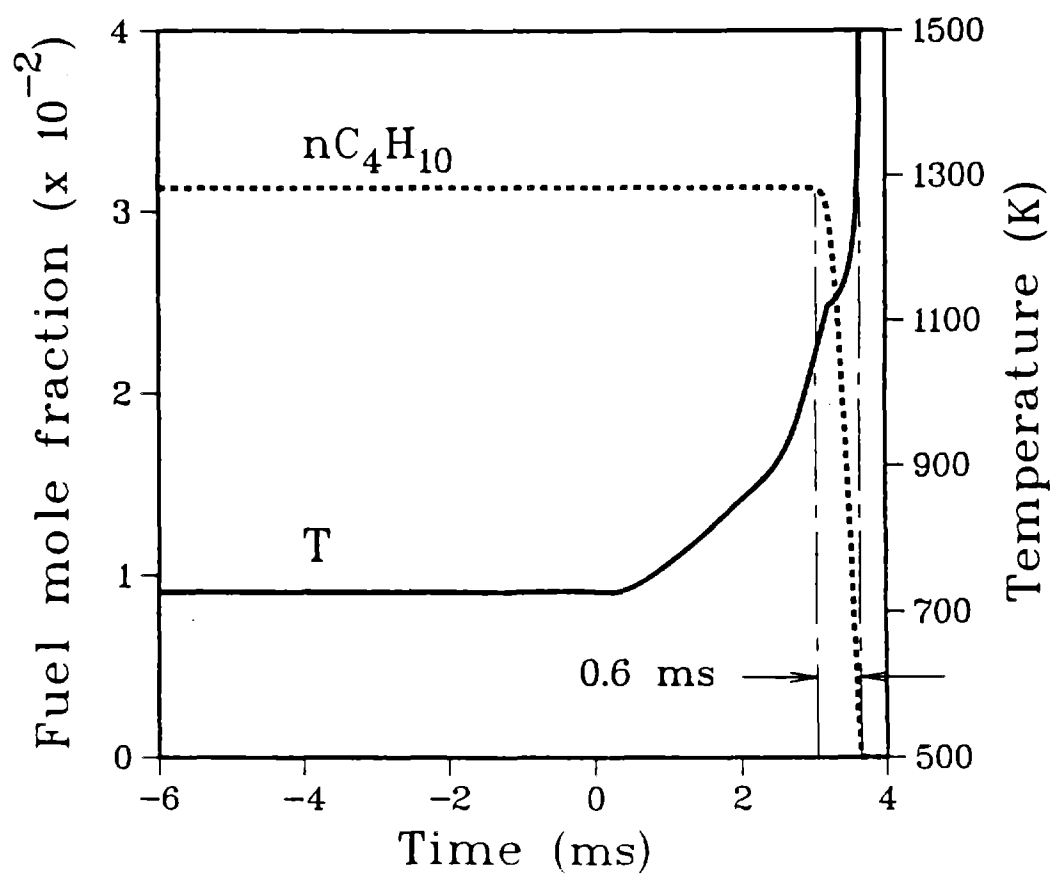


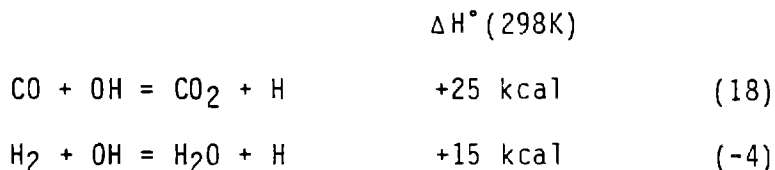
Figure 1b

TDC as reported in Reference 16 which compares well with the measured time of 3.2 ms. The symbols given in Fig. 1a are representative of the temperature data collected by Green and Smith. There was considerable scatter in the data for temperatures below about 800 K [17], and the symbols shown are averages. However, the overall extent of reaction in the calculation did not proceed significantly in this low temperature range. Significant fuel consumption started to occur only when the temperatures in the calculation reached about 1000 K (Fig. 1b). At 1000-1100 K, the Raman temperature measurements have an estimated accuracy of  $\pm 50$ -75 K [16]. More accurate temperature measurements would allow even more stringent tests of the model.

In order to determine whether the model is predicting autoignition to occur in the engine, one needs to compare two characteristic times: the calculated autoignition time of the end gas and the measured flame propagation time in the engine. The flame propagation time is defined as the time required for the flame, initiated by the spark, to consume all the unburned gas in the combustion chamber. If the autoignition time of the end gas exceeds the flame propagation time, the end gas will be consumed by the flame before it has sufficient time to ignite. In Green and Smith's experiment, the flame propagation time was 4.0 ms with spark ignition at TDC. Consequently, when the calculated autoignition times are greater than 4.0 ms after TDC, the model does not predict autoignition in the engine. Under certain conditions, the predicted autoignition times were greater than 4.0 ms. For example, if all the measured temperatures followed during the calculation were artificially lowered by 50 K or more, the calculated autoignition time exceeded 4.0 ms after TDC, and no autoignition was predicted in the engine.

In some of the calculations, the steep temperature rise at autoignition, shown in Fig 1a, never occurred. In these calculations, the reacting mixture was eventually quenched when the temperature and pressure fell during the expansion stroke of the piston. This behavior was predicted when all the measured temperatures followed during the calculation were lowered by 200 K or more. In these cases, the calculation followed the measured temperature, reduced by 200 K or more, until the time of the last measured temperature point. After this time, the calculation proceeded adiabatically with the volume adjusted during the calculation to reproduce the measured pressure. In such cases, the overall extent of reaction never proceeded far enough to achieve autoignition and yield the characteristic temperature rise. The reactions were quenched as the volume expanded and the temperature fell during the expansion stroke.

It is of interest to examine why the characteristic temperature rise at autoignition occurs in some calculations but not in others. This temperature rise occurs when most of the original n-butane has been consumed and the oxidation of CO and H<sub>2</sub> becomes substantial, releasing large quantities of heat:



These reactions are responsible for most of the energy release in autoignition, and they require OH radicals to proceed. In the cases where a characteristic temperature rise does not result, the fuel is not completely consumed. The remaining fuel is much more effective than CO and H<sub>2</sub> at competing for the required hydroxyl radicals [2]:



and prevents the exothermic oxidation of CO and H<sub>2</sub>. Consequently, little heat release takes place in the end gas, and cooling from piston motion eventually reduces the temperature such that the fuel oxidation rate is negligible.

An analysis of the sensitivity of computed autoignition times to individual reaction rates was carried out and the results are displayed in the second column of Table III. The reactions are listed in order of their importance based on their sensitivity values. Each sensitivity listed was determined by increasing an individual reaction rate by a factor of two and recording the change in autoignition time. The sensitivities are defined:

$$\text{sensitivity} = \frac{\tau - \tau_{\text{ref}}}{\tau_{fu}} \times 100$$

where  $\tau$  is autoignition time when a reaction rate is increased,  $\tau_{\text{ref}}$  is the reference autoignition time with unaltered reaction rates, and  $\tau_{fu}$  is the characteristic fuel disappearance time.  $\tau_{fu}$  is defined as the interval between the time where one percent of the fuel has been consumed and the time of autoignition. For the reference case,  $\tau_{fu}$  is 0.6 ms as indicated in Fig. 1b. The sensitivities here are based on  $\tau_{fu}$  since it is only during this time that significant fuel consumption occurs. For time prior to  $\tau_{fu}$ , the amount of fuel oxidation is negligible. The results of the sensitivity analysis are discussed later.

## 2. Calculations following only the measured pressure.

In the next series of calculations, the reactions in a sample of n-butane/air mixture were traced from a much earlier time in the engine cycle. In a typical engine, the end gas spends a considerable time at

Table III

Reaction rate sensitivity

<u>Reaction</u>		<u>Constant volume (1000 K)</u>	<u>Follow T and P</u>	<u>Follow P only</u>
$C_4H_{10}+HO_2$	$= C_4H_9+H_2O_2$	-32	-26	-22
$H_2O_2+M$	$= OH+OH+M$	-28	-12	-12
$HO_2+HO_2$	$= H_2O_2+O_2$	26	22	16
$CH_3+HO_2$	$= CH_3O+OH$	-9	-18	-13
$R+O_2$	$= \text{olefin}+HO_2$	-1	-12	-8 <sup>a</sup>
$H+O_2$	$= OH+O$	-1	-10	-7
$R+O_2$	$= RO_2$	-4	-9	-6 <sup>b</sup>
$C_4H_{10}+OH$	$= C_4H_9+H_2O$	-1	-4	-2
$C_4H_{10}+H$	$= C_4H_9+H_2$	0 <sup>c</sup>	3	2
$H+O_2+M$	$= HO_2+M$	0	-2	-1

---

R = CH<sub>3</sub>, C<sub>2</sub>H<sub>5</sub>, nC<sub>3</sub>H<sub>7</sub>, iC<sub>3</sub>H<sub>7</sub>, pC<sub>4</sub>H<sub>9</sub>, sC<sub>4</sub>H<sub>9</sub>

<sup>a</sup> R does not include CH<sub>3</sub> in this case.

<sup>b</sup> rate increased in the forward direction only.

<sup>c</sup> zero indicates less than 0.5% change



temperatures in the range of 450 to 900 K where low temperature reaction paths may be important (about 49 ms at 600 rpm in the engine used by Green and Smith, as shown in Fig. 2). In this reference case, the calculation began at bottom dead center so that the lower temperature portions of the engine cycle were included and the role of low temperature reactions could be assessed. The fuel/air mixture was initially at 450 K and 0.9 atm. The pressure of 0.9 atm at bottom dead center was estimated by using the manifold pressure (1.5 atm) and assuming a volumetric efficiency of 0.6. Starting with these initial conditions, the calculation followed reactions in the mixture, adjusting the volume to match the measured pressure. Heat losses from the end gas to the surroundings were not included, except in the manner that they affected the measured pressure which was followed during the calculation. The temperature that resulted from the model depended on heat release in the mixture and changes in volume to match the measured pressure. For the time period between bottom dead center and 13 ms ( $50^\circ$ ) before TDC, the pressure was estimated by an adiabatic, isentropic expression based on piston motion since the pressure during these times was too low to be accurately measured by the available pressure gauge. As shown in Fig. 2, the temperature history that resulted from this calculation intersected some of the measured temperature points which were followed in the previous case. The calculated temperatures were higher than the measured temperatures during the period of time between 3 ms before TDC and TDC. This discrepancy may be due to heat losses from the end gas that were not included in this modeling treatment or due to some uncertainty in the Raman temperature measurements which are less accurate for temperatures below 800 K.

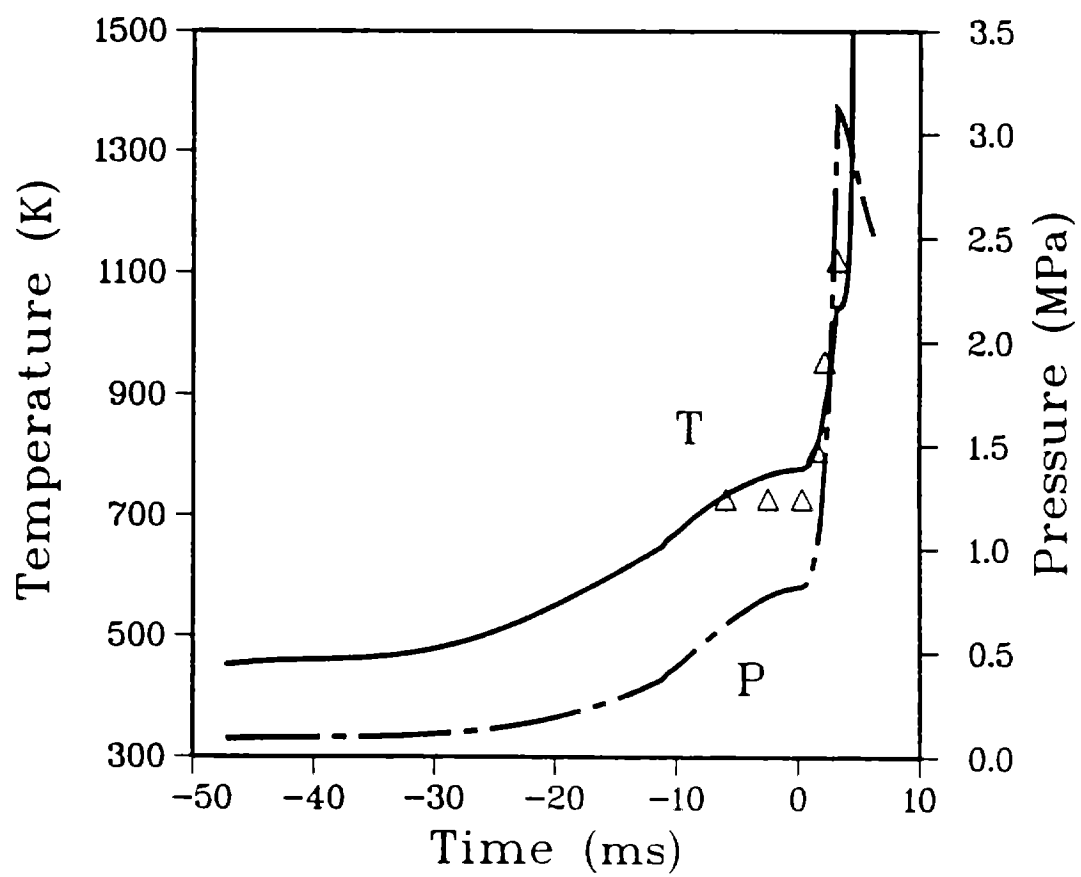


Figure 2

Using the above treatment, the predicted autoignition time was 4.38 ms compared to 3.6 ms predicted previous treatment when both the temperature and pressure histories were followed by the calculation (the experimental measured time was 3.2 ms). The previous treatment is probably a more accurate description since heat transfer from the end gas to the surroundings was taken into account by following the measured temperature. When the engine is operating under knocking conditions, the temperature of combustion chamber walls tends to be rather high, and some preheating of the fuel/air charge may occur during the compression phase of the engine cycle. A treatment which follows the measured temperature will take this preheating into account and would tend to predict a faster autoignition time.

The sensitivity of the autoignition time to changes in various reaction rates was determined for this modeling treatment, and the sensitivity constants are presented in the right-hand column of Table III. The sensitivities in this case are defined as before.

Calculations were run with and without the inclusion of an additional set of reactions that tend to be important at low temperatures (Table II). With the low temperature reactions of Table II excluded from the calculation, the autoignition time was 4.43 ms after TDC. When the reactions of Table II were combined with that of Table I, the autoignition time was 4.38 ms. Using the sensitivity scale of Table III, this corresponds to an 8 percent relative decrease in autoignition time when the low temperature reactions were included. This 8 percent value, obtained when including all the 85 reactions of Table II, would rank fifth in the sensitivity table and would not be a large sensitivity compared to the other higher values obtained by changing one reaction rate by a factor of

two. A 22 percent relative decrease in autoignition time is produced by increasing



by only a factor of two. Consequently, compared to other key reactions, the low temperature reactions of Table II do not have a large influence on autoignition times for n-butane/air mixtures at these conditions.

### 3. Constant volume calculations.

An even more simplified approach in the characterization of autoignition is to invoke the constant volume assumption. With the appropriate choice of initial temperature and pressure, the calculations exhibit primary reaction paths that are very similar to those identified by the previous, more complex calculations. In these calculations, autoignition of a stoichiometric, n-butane/air mixture at constant volume and an initial pressure of 30 atm was examined with no heat losses allowed from the mixture to the surroundings. The initial pressure was chosen to be approximately that which the end gas experiences just prior to autoignition in the engine. During the induction period of these calculations, the mixture remains at a nearly constant temperature for a relatively long period of time, followed by a steep rise in temperature indicating that ignition has taken place. As a result of this simplified treatment, the variation in temperature and pressure in the engine cycle is not modeled. This approach is useful in defining characteristic temperatures and pressures for autoignition of the end gas. Characteristic autoignition times at different initial temperatures are given in Fig. 3.

Two series of calculations were made: one series employing the high temperature reactions only (Table I) and the other series including both

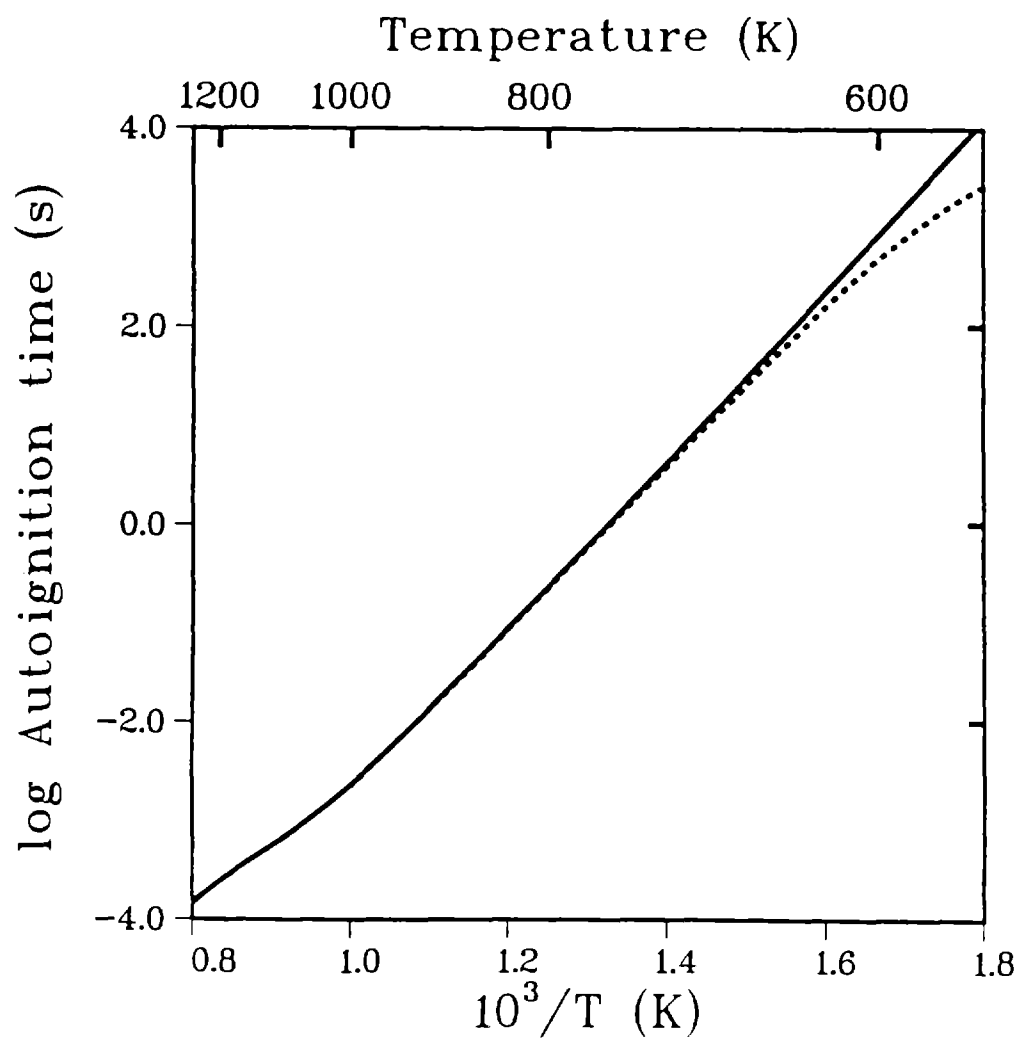


Figure 3

the high and low temperature mechanisms combined (Table I and II). For  $T \leq 650$  K, the characteristic autoignition time is affected by the low temperature paths; however, the autoignition times in this temperature regime are very long and are three to four orders of magnitude greater than the time available for autoignition in a spark ignition engine. Only when the initial temperature is above about 1000 K are the characteristic times in the order of magnitude of milliseconds, which is the approximate time needed to obtain autoignition in the engine.

The sensitivity of the autoignition time to changes in various reaction rates for the constant volume calculations was calculated and the constants are given in the first column of Table III. In these cases, the sensitivity is defined as  $100(\tau - \tau_{\text{ref}})/\tau_{\text{ref}}$ .

## DISCUSSION

The chemical kinetic reactions for which the autoignition calculations show sensitivity are discussed in this section. In Table III, the reactions are ranked in the order of their sensitivity levels starting with the highest level. As already noted, the sensitivity values are defined in terms of computed autoignition times. Negative sensitivities indicate that an increase in a particular reaction rate results in a reduction in the autoignition time by raising the overall rate of fuel oxidation, while positive values indicate that the rate increase lengthens the autoignition period and lowers the overall rate of fuel oxidation.

The predominant feature of Table III is that for all three families of calculations shown, autoignition was most sensitive to reactions involving the production and consumption of  $\text{HO}_2$  and  $\text{H}_2\text{O}_2$ . Autoignition times were most affected by the rate of



The  $\text{H}_2\text{O}_2$  produced here decomposes and promotes chain branching through



Reactions 194 and 195 followed by Reaction 13 provide the dominant chain branching path found at temperatures and pressures where the end gas tends to knock. This result contrasts with the behavior of hydrocarbon-air systems at lower pressures ( $P \approx 1$  atm) and higher temperatures ( $T \geq 1000$ ) where the chain branching reaction



predominates [2]. As seen in the sensitivity ranking given in Table III, this latter chain branching path, Reaction 1, is not particularly important at the present conditions of higher pressure (20-30 atm) and lower temperature (500-1100 K). This reduced importance can be attributed to the recombination reaction

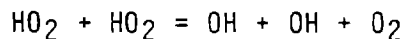


which competes effectively at elevated pressure with Reaction 1 for H atoms and promotes chain branching as described above.

As discussed above,  $\text{HO}_2$  can react with the fuel (194,195) and promote chain branching. An alternative to this path is self-reaction of  $\text{HO}_2$

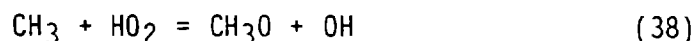


This path is chain propagating since the  $\text{H}_2\text{O}_2$  product decomposes fairly rapidly (Reaction 13) and yields the net path

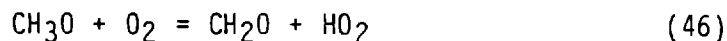


Increasing the rate of Reaction -12 significantly slows the overall fuel oxidation rate (Table III), since this chain propagating path is being enhanced at the expense of the previous chain branching path (Reactions 194, 195 followed by 13).

Finally, autoignition calculations were sensitive to the rate of



Most of the methoxy formed reacts with  $\text{O}_2$ :



This sequence converts the relatively unreactive  $\text{CH}_3$  radical into a much more reactive OH radical, accelerating the autoignition process.

The sensitivity results (Table III) for the constant volume calculation are very similar to those for the calculations which follow measured pressure and both measured pressure and temperature. These constant volume calculations were performed at an initial temperature and pressure of 1000 K and 30 atm. With the appropriate choice of characteristic temperature and pressure, these simple calculations with short computational times show the similar trends as the more complex calculations which follow temperatures and pressures and have long computational times. The series of reactions responsible for fuel oxidation is somewhat different at the higher pressures and lower temperatures encountered in the end gas compared to the atmospheric pressure and somewhat higher temperatures ( $T \geq 1000$  K) of many combustion systems [2,5]. In the end gas, reactions between the fuel and  $\text{HO}_2$  tend to be much more important. The primary reactions consuming the fuel in the end gas environment are:



These are listed in descending order of their contribution to fuel consumption. Reactions 182 and 183 with OH radicals are the dominant paths



for fuel consumption. Reactions 194 and 195 involving  $\text{HO}_2$  contribute significantly to fuel consumption during the early stages of fuel oxidation, and their contribution diminishes at later times. Autoignition times are very sensitive to this path, since it leads to chain branching through Reaction 13. Fuel reactions involving  $\text{CH}_3$ ,  $\text{CH}_3\text{O}$ , and  $\text{H}$  radicals make only minor contributions to fuel consumption. The effect of equivalence ratio  $\phi$  on the above ranking of radical-fuel reactions is small for  $0.5 \leq \phi \leq 1.5$ .

The butyl radicals resulting from the above abstraction reactions can either react with  $\text{O}_2$  or thermally decompose:



At the high pressures considered here, the bimolecular path is favored, and most of the butyl radicals are consumed by  $\text{O}_2$ , producing butene.

Significant amounts of butene have been measured in the end gas of an engine operating on n-butane/air [24]. These measurements compare well with relative amounts of butene predicted in the end gas by our chemical kinetic model [24]. However, previous modeling calculations and measurements in a flow reactor indicated only small amounts of butene [5]. The flow reactor experiments were run with dilute mixtures of n-butane/ $\text{O}_2$  in nitrogen at a pressure of 1 atm and a temperature of approximately 1000 K. Under these low pressure conditions with dilute fuel/ $\text{O}_2$  mixtures, the decomposition route dominates and almost no butene is produced.

## ADDITIVES

Fuel additives can inhibit engine knock, thereby extending fuel octane values. Tetraethyl lead (TEL) is one of the most effective anti-knocks agents, but its usage has been severely restricted due to environmental constraints. An understanding of the specific inhibitory mechanism of TEL and related anti-knock compounds might aid the development of new, alternative additives that are environmentally acceptable. Also, this understanding may give an general approach to controlling knock that suggests strategies which do not involve additives.

Most investigators believe that TEL thermally decomposes in the end gas and oxidizes to form lead oxide [26,27,28]. However, the details of the chemical and physical processes by which lead oxide forms are not very well understood. Additionally, the question of whether the lead oxide in the end gas is a vapor or solid is controversial [28]. In this study, TEL was assumed to form lead oxide particles. These particles are believed to react heterogeneously with radicals or other pro-knock species and suppress autoignition [26,27].

The previously discussed calculations demonstrated the sensitivity of computed autoignition times to reactions producing and consuming  $\text{HO}_2$  and  $\text{H}_2\text{O}_2$ . This result suggests that an additive which reduces the concentrations of  $\text{HO}_2$  and  $\text{H}_2\text{O}_2$  could significantly inhibit autoignition by providing competition for these species and retarding the chain-branching path of Reactions 194 and 195 followed by 13. Cheaney et al.[27] have presented evidence that  $\text{HO}_2$  and  $\text{H}_2\text{O}_2$  react on lead oxide surfaces. In the calculations described below, surface reactions between TEL and species such as  $\text{HO}_2$  or  $\text{H}_2\text{O}_2$  are postulated to assess their effect on autoignition times and to evaluate possible modes of action

of TEL. Possible removal by TEL of radical species such as OH, H, and O is also examined.

In the calculations performed, the lead oxide or other anti-knock particles are assumed to facilitate the conversion of a reactive species into relatively unreactive products. For conversion of  $\text{H}_2\text{O}_2$  on a surface,

$$\begin{aligned} \text{H}_2\text{O}_2^{\text{surf}} &= \text{unreactive products} \\ \text{rate} &= k_{\text{surf}} [\text{H}_2\text{O}_2] \end{aligned} \quad \text{Eqn. 1}$$

where  $k_{\text{surf}}$  is the rate constant for surface reactions occurring on the particles. The surface reaction rate is estimated from simple kinetic theory of gases:

$$k_{\text{surf}} = r(\text{surf}/\text{vol})\sqrt{(kT/2\pi m)} \quad \text{Eqn. 2}$$

where  $r$  is the efficiency of  $\text{H}_2\text{O}_2$  removal upon collision with a solid particle;  $\text{surf}/\text{vol}$  is the total amount of particle surface area per unit gas volume; and  $m$  is the mass of an  $\text{H}_2\text{O}_2$  molecule. Inherent in Eqn. 2 is the assumption that the rate of diffusion of  $\text{H}_2\text{O}_2$  through the surrounding gases is not rate limiting. The diffusion of  $\text{H}_2\text{O}_2$  to the lead oxide particles is rapid since the average particle spacing is so small, about  $1 \mu\text{m}$  (for a number density of  $2 \times 10^{17} \text{ m}^{-3}$  which is obtained later). The characteristic time for  $\text{H}_2\text{O}_2$  diffusion to the lead oxide particles is about  $0.01 \mu\text{s}$  compared to characteristic fuel disappearance time of about  $600 \mu\text{s}$ . The major uncertainty in calculating  $k_{\text{surf}}$  is in the product  $r(\text{surf}/\text{vol})$  whose value is estimated in the following paragraphs.

The particle surface area per unit volume in the combustion chamber,  $\text{surf}/\text{vol}$ , can be estimated from the average surface area of a lead oxide particle and their number density. Graiff [28] sampled lead oxide particles from the end gas of a spark ignition engine over a range of

compression ratios. The particles are very small, 4-10 nm diameters. This characteristic of lead oxide may account for its high degree of effectiveness. The production of very small particles results in large total surface areas in the end gas and leads to high surface reaction rates. Using the particle diameters measured by Graiff and assuming perfectly spherical particles, a surface area of  $1.5 \times 10^{-16} \text{ m}^2$  is obtained for an average particle of 7 nm diameter. This area could be larger if the surface of the lead oxide particles is irregular.

The lead oxide number density can be calculated for the typical case of 3 gm TEL per gallon of gasoline as follows:

$$\frac{\text{mass PbO}}{\text{mass mixture}} = \frac{\text{mass PbO}}{\text{mass gasoline}} \times \frac{\text{mass gasoline}}{\text{mass mixture}} \quad \text{Eqn. 3}$$

Using the ratio of the molecular weights for TEL and lead oxide, and an average density of gasoline (3.0 kg/gallon), one obtains  $6.9 \times 10^{-4}$  for the first term on the right hand side; for the second term, a typical air/fuel mass ratio of 15 for gasoline implies a value of  $6.3 \times 10^{-2}$ . This gives a mass ratio of lead oxide to fuel-air mixture of  $4.3 \times 10^{-5}$ . One can convert from a mass ratio to a volume ratio by employing the fuel-air mixture density near TDC (about  $9 \text{ kg/m}^3$ ) and the density of lead oxide ( $9 \times 10^3 \text{ kg/m}^3$ ). The result is that the ratio of volume of solid lead oxide particles to the total gas volume is  $4.3 \times 10^{-8}$ . Finally, using an average particle diameter of 7 nm and assuming spherical particles, one obtains a lead oxide number density of  $2.4 \times 10^{17} \text{ m}^{-3}$ . Combining the number density with the previously obtained particle surface area, one gets the lead oxide surface area to per unit gas volume,  $\text{surf/vol} = 40 \text{ m}^{-1}$ .

This ratio of total surface area of the lead oxide particles to the total gas volume,  $\text{surf/vol}$ , could be much higher. This can be seen by reexamining the above estimate as follows. The approximate volume of lead oxide in the end gas is given by the amount of TEL in the fuel. Next, the assumption is made that the total volume of lead oxide is distributed among a number of perfectly spherical particles. However, a sphere has the smallest surface area for its inherent volume. An irregular shape may give much more surface area for a given particle volume. By choosing a spherical shape, one is considering the case of minimum estimated surface area.

The next quantity required to calculate the surface reaction rate is the surface efficiency,  $\tau$ . The authors have been able to find little information regarding the efficiencies of radicals and hydroperoxides reacting on lead oxide surfaces. Information is available for some radical species such as H and O atoms on surfaces other than lead oxide. H atoms have a value of  $\tau$  on platinum and nickel that is very high and close to one [29,30]. O atoms also have high efficiencies on metal surfaces [31]. For  $\text{HO}_2$  and  $\text{H}_2\text{O}_2$ , no information on efficiencies was found. Since lead oxide is one of the most effective anti-knocks and experimental evidence suggests it acts through surface reactions, it probably has a very efficient catalytic surface. In the subsequent calculations, a unit efficiency was used for each species that was considered to participate in surface reactions. These calculations were used to assess the relative impact on autoignition times of a particular species' participation in surface reactions.

No provision was made in the model to account for the ethyl radicals contained in TEL. The mechanism of conversion of TEL to lead oxide is

poorly understood and more research is required in this area. The effect on the calculation of neglecting the ethyl radicals is dependent on the mechanism by which they are separated from TEL and the time that this separation occurs. Under some conditions, the ethyl radicals in TEL may tend to promote knock.

Autoignition calculations were performed which included the effect of surface reactions using the above formulation. These calculations identified the species which may participate in surface reactions and significantly affect autoignition times. Autoignition times were calculated using the autoignition model which followed the measured pressure, but not the measured temperatures (i.e. approach 2 discussed earlier). This autoignition model had the advantage of covering the temperature history of the entire compression stroke. For all the species whose removal was considered, inclusion of surface reactions either inhibited the autoignition process or had no significant effect. The change in autoignition time due to surface reactions was referenced to the characteristic fuel disappearance time ( $\tau_{fu}$ ) for the case when no surface reactions were present. The results for removal of various radical species and hydroperoxides are given in Table IV in terms of relative changes in autoignition times. Removal of  $H_2O_2$  by surface reactions had the greatest effect on autoignition times. Similarly, autoignition times were very sensitive to  $HO_2$  removal. Specific removal of other species considered ( $CH_3O_2$ ,  $C_2H_5O_2$ ,  $C_4H_9O_2$ ,  $C_4H_9OOH$ ,  $OH$ ,  $H$ ,  $O$ ) by surface reactions affected autoignition times only slightly.  $H_2O_2$  and  $HO_2$  are the only species whose removal affects autoignition times significantly. This result is attributed to two factors. The surface reaction rate (Eqn. 1) is directly proportional to the species

Table IV

Effect of surface reactions on autoignition times

	Increase in autoignition time [percent]	Mole fraction at $\tau_{fu}/2$ [ $\times 10^{-6}$ ]
$H_2O_2 + HO_2$	31	-
$H_2O_2$	23	160
$HO_2$	11	40
$RO_2$	0.7 <sup>a</sup>	-
$CH_3O_2$	0.6	3
$C_2H_5O_2$	0 <sup>b</sup>	0.2
$C_4H_9O_2$	0	0.07
OH, H, O	0	< 0.08
$C_4H_9OOH$	0	0.0005

---

<sup>a</sup> R =  $C_4H_9$ ,  $C_3H_7$ ,  $C_2H_5$ ,  $CH_3$

<sup>b</sup> zero means less than 0.1 %

concentration and is highest for the species with the largest concentration. The concentrations of  $\text{H}_2\text{O}_2$  and  $\text{HO}_2$  significantly exceed those of the other species examined considered. This can be seen in the right-hand column of Table IV where the concentrations of each species at the mid-point of the fuel disappearance period are listed for comparison. Secondly, the sensitivity study discussed previously identified reactions involving  $\text{HO}_2$  and  $\text{H}_2\text{O}_2$  as being the most influential on autoignition times. Surface reactions that remove these species compete with chain-branching reactions and slow the autoignition process.

The effect of TEL concentration on autoignition times was examined. In this simplified model of TEL, the impact of changing the TEL concentration is seen by a change in  $\text{surf/vol}$  which then affects the surface reaction rate constant,  $k_{\text{surf}}$ . A doubling of the TEL concentration would double the surface reaction rate in this treatment. When the TEL concentration was increased by a factor of two in the model, the autoignition time was retarded by about twice the previous amount.

For some fuels, such as alcohols, TEL may act as a promoter of knock rather than an inhibitor [32]. The modeling treatment described here cannot account for this effect. Autoignition calculations were performed with methanol as a fuel, and the results showed that addition of surface reactions involving  $\text{HO}_2$  and  $\text{H}_2\text{O}_2$  increased the autoignition time. The inability of the model to explain TEL addition to methanol may be due to neglecting the ethyl radicals in TEL or more likely, due to some process not controlled by chemical kinetics.

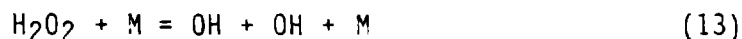
This is a simplified treatment of the effect of TEL addition to n-butane/air mixtures, but the results of the calculations do exhibit the



expected inhibitory effect. The approach also provides a relative ranking of the impact of various species participation in surface reactions. Further clarification is needed in a number of areas in order to make more accurate estimates. The surface reaction rate is dependent on the value of the efficiency,  $\Gamma$ , and on the total particle surface area both which contain significant uncertainties. Experimental measurements of  $\Gamma$  for  $H_2O_2$  and  $HO_2$  reacting on metal oxide surfaces at high pressure are needed. Additional data are also required on the size distribution and shape of the lead oxide particles.

## CONCLUSIONS

Modeling of autoignition of n-butane/air mixtures identified the reaction sequence



as being the dominant path that provides chain branching at the high pressures encountered in the end gas. Also, a set of reactions that describes the addition of oxygen to alkyl radicals and their subsequent formation of alkyl hydroperoxides was included in the mechanism to better describe chemical kinetic behavior at low temperatures. Inclusion of this set of reactions had no significant effect on the autoignition times calculated at end gas conditions. Additional work needs to be performed to examine isomerization reactions of alkyl peroxy radicals and to assess their effect on autoignition times, factors which are expected to be significant for fuel molecules larger than the n-butane used in this study. The addition of TEL to n-butane/air mixtures was examined at conditions found in the end gas. TEL was assumed to form lead oxide

particles which promote removal of radicals through surface reactions.  $\text{HO}_2$  and  $\text{H}_2\text{O}_2$  were the only radicals whose removal had a significant effect on autoignition times. This result suggests that TEL inhibits autoignition by leading to removal of  $\text{HO}_2$  and/or  $\text{H}_2\text{O}_2$  from the end gas.

#### ACKNOWLEDGMENTS

The authors gratefully acknowledge Drs. R.M. Green and J.R. Smith of Sandia National Laboratory for many useful discussions and for the use of their experimental data. Dr. Peter Jessup of Union Oil provided valuable assistance in estimating lead oxide concentrations in engines. Helpful discussions with Professor Nicholas P. Cernansky of Drexel University, Professor Frederick L. Dryer of Princeton University and Professor A.K. Oppenheim of University of California, Berkeley are very much appreciated. This work was performed under the auspices of the U.S. Department of Energy by the Lawrence Livermore National Laboratory under contract No. W-7405-ENG-48.

#### REFERENCES

1. Leppard, W.R., Combust. Sci. Tech., 43:1 (1985).
2. Westbrook, C.K. and Dryer, F.L. Prog. Energy Combust. Sci. 10:1-57 (1984).
3. Dimpelfeld, P.M., and Foster, D.E. The prediction of autoignition in a spark ignited engine. To appear as an SAE paper, 1984
4. Westbrook, C.K. and Pitz, W.J. Combust. Sci. Tech. 37:117 (1984).
5. Pitz, W.J., Westbrook, C.K., Proscia, W.M. and Dryer, F.L., A comprehensive chemical kinetic reaction mechanism for the oxidation of n-butane, Twentieth Symposium (International) on Combustion, The Combustion Institute, Pittsburgh, PA, 1984.

6. Halstead, M.P., Kirsh, L.J. and Quinn, C.P. Combust. Flame 30:45 (1977).
7. Natarajan, B. and Bracco, F.V. Combust. Flame 57:179 (1984).
8. Carrier, G., Fendell, F., Fink, S. and Feldman, P., Combust. Sci. Tech. 38:1 (1984).
9. Dale, J.D., and Oppenheim, A.K., SAE Paper 820047, 1982.
10. Gussak, L.A., Karpov, V.P., and Tikhonov, Yu. V. SAE Paper 790692, 1979.
11. Lund, C.M. HCT - a general computer program for calculating time-dependent phenomena involving one-dimensional hydrodynamics, transport, and detailed chemical kinetics. Lawrence Livermore National Laboratory, Livermore, CA, report UCRL-52504, 1978.
12. JANAF Thermochemical Tables, U.S. Government Printing Office, Washington, D.C., 1971.
13. Bahn, G.S. NASA report NASA-CR-2178, 1973.
14. Benson, S.W. Thermochemical Kinetics, Wiley, New York, 1976.
15. Pitz, W.J., and Westbrook, C.K. Chemical kinetics modeling of engine knock: preliminary results. Presented at the Western States Section of the Combustion Institute, Fall meeting, 1983.
16. Green, R.M., and Smith, J.R. An experimental study of engine knock. Presented at the Western States Section of the Combustion Institute, Spring meeting, 1984.
17. Smith, J.R., Green, R.M., Westbrook, C.K., and Pitz, W.J. An experimental and modeling study of engine knock. Twentieth Symposium (International) on Combustion, The Combustion Institute, Pittsburgh, PA, 1984.
18. Obert, E.F., Internal Combustion Engines and Air Pollution, Harper and Row, Publishers, Inc., New York, 1973, p.234-235.
19. Downs, D., Walsh, A.D. and Wheeler, R.W. Phil. Trans. Roy. Soc., A 243:463 (1951).
20. Kaiser, E.W., Westbrook, C.K., and Pitz, W.J. Acetaldehyde oxidation in the negative temperature coefficient regime: Experimental and modeling results. Presented at the Western States Section of the Combustion Institute, Fall meeting, 1984. Submitted for publication.
21. Benson, S.W. Oxidat. Comm. 3:169 (1982).
22. Baldwin, R.R., Matchan, M.J., and Walker, R.W. Combust. Flame 15:109 (1970).
23. Griffiths, J.F., and Hasko, S.M. Proc. R. Soc. Lond. A 393:371 (1984).

24. Cernansky, N.P., Green, R.M., Pitz, W.J., and Westbrook, C.K. On the low temperature chemistry preceding end gas autoignition. To be presented at the national meeting of the American Chemical Society, Chicago, September 8-13, 1985.
25. Leppard, W.R. Private communication, 1985.
26. Walsh, A.D., in Six Lectures on the Basic Combustion Process, Ethyl Corporation, Detroit, Michigan, 1954, p.102-125.
27. Cheaney, D.E., Davies, D.A., Davis, A., Hoare, D.E., Protheroe, J., and Walsh, A.D. Seventh Symposium (International) on Combustion, The Combustion Institute, Pittsburgh, PA, p. 183, 1959.
28. Graiff, L.B. SAE Paper 660780, 1966.
29. Smith, W.V. J. Chem. Phys. 11:110 (1943).
30. Katz, S., Kistiakowsky, G.B., and Steiner, R.F. J. Amer. Chem. Soc. 71:2258 (1949).
31. Marsden, D.G.H. and Linnett, J.W. Fifth Symposium (International) on Combustion, The Combustion Institute, Pittsburgh, PA, p. 685, 1955.
32. Pischinger, F.F. In discussion of paper by S.L. Hirst and L.J. Kirsch in Combustion Modeling in Reciprocating Engines (J.N. Mattavi and C.A. Amann, Ed.), Plenum Press, New York, London, 1980, p. 224.

#### FIGURE CAPTIONS

- 1a. Pressure and temperature histories of the end gas. Time is relative to spark ignition. (— calculated temperature;  $\Delta$  measured temperatures and — — pressure both of Green and Smith [16,17]; engine speed, 600 rpm; manifold temperature, 423 K; manifold pressure, 1.5 atm absolute)
- 1b. Calculated fuel concentration and temperature in end gas.
2. Temperature and pressure histories in the end gas when calculation follows the measured pressure only. (— calculated temperature;  $\Delta$  measured temperature and — — pressure, both from Reference 16).
3. Autoignition times for stoichiometric, n-butane/air at constant volume and an initial pressure of 30 atm. Chemical kinetic reaction mechanisms used: — Table I only, — — both Table I and Table II.